Electroweak multi-monopoles

Romain Gervalle[1,*] and Mikhail S. Volkov[1,†]

[1] *Institut Denis Poisson, UMR - CNRS 7013,*

Université de Tours, Parc de Grandmont, 37200 Tours, France

arXiv:2211.04875v1 [hep-th] 9 Nov 2022

We construct the multi-charge generalizations for the electroweak magnetic monopole solution of Cho and Maison within a wide range of values of the magnetic charge. We use the same ansatz for the axially symmetric fields as the one previously employed to construct the electroweak sphalerons and compare the internal structure of monopoles with that of sphalerons. The monopoles have zero dipole moment but a finite quadrupole momentum that rapidly increases with growing magnetic charge. For large charges, the monopole configurations are strongly squashed and show inside a bubble of symmetric phase filled with a U(1) hypercharge field produced by a pointlike magnetic charge at the origin, strong enough to suppress all other fields and restore the full gauge symmetry. The bubble is surrounded by a large belt of broken phase containing a magnetically charged ring filled with a nonlinear W-condensate, squeezed between two superconducting rings of opposite electric currents. In the far field region there remains only the magnetic field supported by the total magnetic charge contained at the origin and in the magnetic ring. The axially symmetric monopoles are probably just a special case of more general monopole solutions not possessing any continuous symmetries. The Cho-Maison monopole is stable but the stability of its multi-charge generalizations is not yet confirmed. All electroweak monopoles have infinite energy due to the pointlike U(1) charge at the origin, but the energy is expected to become finite after taking gravity into account, which should provide a cutoff via creating an event horizon to shield the U(1) charge.

* romain.gervalle@univ-tours.fr

† volkov@lmpt.univ-tours.fr

Contents

I. INTRODUCTION 3

II. ELECTROWEAK THEORY 6

III. AXIAL SYMMETRY 9
A. Removing string singularity in the monopole case 11
B. Removing string singularity in the sphaleron case 12
C. Fixing the gauge 13

IV. SPHERICALLY SYMMETRIC SOLUTIONS 13
A. Monopoles 13
1. Abelian monopoles of Dirac 14
2. The non-Abelian monopole of Cho and Maison 16
B. Sphaleron 17

V. AXIALLY SYMMETRIC MONOPOLES 18
A. Virial relation 20
B. Solutions 21
C. The interior structure 23
D. Quadrupole moment 26
E. The limit of large magnetic charge 27

VI. SPHALERONS AND THEIR INTERNAL STRUCTURE 32

VII. SUMMARY AND CONCLUDING REMARKS 35

A. FAR FIELD ZONE 38
1. Higgs sector 39
2. Electromagnetic and Z sectors 39
3. W sector 40
a. Monopoles 40
b. Sphalerons 42

B. SOLUTION AT THE ORIGIN 42

References 45

I. INTRODUCTION

The magnetic monopole in the U(1) electrodynamics is described by the Coulombian magnetic field, $\vec{\boldsymbol{\mathcal{B}}} = \boldsymbol{P}\vec{\boldsymbol{r}}/\boldsymbol{r}^3$. As was noticed by Dirac [1] (see also [2]), although one cannot find a globally regular vector potential $\vec{\boldsymbol{\mathcal{A}}}$ such that $\vec{\boldsymbol{\mathcal{B}}} = \vec{\nabla} \wedge \vec{\boldsymbol{\mathcal{A}}}$, one can use two locally regular potentials related to each other via a gauge transformation in a transition region. This imposes the quantization condition for the magnetic charge,

$$\boldsymbol{P} = \frac{\boldsymbol{\hbar c}}{2\boldsymbol{e}} \times n, \qquad n = \pm 1, \pm 2, \ldots \tag{1.1}$$

Extending the gauge group to SU(2) and adding a Higgs field in the adjoint representation, allows one to obtain monopoles described by a globally regular potential and without the central singularity, as was noticed by t'Hooft [3] and by Polyakov [4]. These monopoles have a finite energy and contain massive fields in the central region, while at large distances only the massless U(1) gauge field survives and approaches that of the Dirac monopole. This discovery triggered a large number of theoretical studies (see [5–9] for reviews and, e.g., [10, 11] for particular aspects of monopoles), but the experimental search for magnetic monopoles has always been giving negative results (see [12–14] for recent reviews). One of the explanation for this is the fact that the t'Hooft-Polyakov monopoles are not described by the Standard Model, because the latter contains in the electroweak sector the Higgs field in the fundamental and not adjoint representation. As a result, the standard topological arguments [8] for the existence and stability of monopoles do not apply.

One may wonder then if there are any magnetic monopoles in the electroweak theory at all ? The answer is of course positive because the Dirac monopoles should be solutions of the theory containing the U(1) electrodynamics as a special limit. Another type of electroweak monopoles was described by Nambu [15], who noticed that the electroweak theory contains vortex solutions similar to the Abrikosov-Nielsen-Olesen vortices in the Abelian Higgs model [16, 17]. Unlike the latter, however, the electroweak vortices can terminate, and then the magnetic flux trapped inside the vortex comes out through the termination point and spreads out all over the space, which imitates the magnetic monopole. To describe this, Nambu used the "isospinor" form for the Higgs field,

$$\Phi_{\rm mon} = \phi \begin{pmatrix} \sin\frac{\vartheta}{2}\, e^{-i\varphi} \\ -\cos\frac{\vartheta}{2} \end{pmatrix}, \tag{1.2}$$

which is ill-defined at the negative part of the z-axis since it has no limit for $\vartheta \to \pi$. To cure this, Nambu assumed that the amplitude ϕ vanishes at $\vartheta = \pi$, thereby producing a

semi-infinite vortex extending along the negative part of the z-axis and terminating at the monopole at $z = 0$. Analyzing the fields inside the vortex and those spreading out to infinity through the vortex termination, Nambu arrived at the following expression for the magnetic charge,

$$\boldsymbol{P} = \frac{\boldsymbol{\hbar c}}{\boldsymbol{e}} \times \sin^2 \theta_{\rm W} \,, \tag{1.3}$$

where $\theta_{\rm W}$ is the weak mixing angle. This corresponds to the Dirac value (1.1) for $n = 2$ but with the additional factor of $\sin^2 \theta_{\rm W}$ (in general the charge can be an integer multiple of (1.3)). If the vortex is semi-infinite, then the resulting system has an infinite energy and cannot be static since the vortex will be pulling the monopole. However, the vortex may have a finite length and terminate some distance away on an antimonopole, then the resulting monopole-antimonopole pair will have a finite energy and will be spinning around the common center of mass [18].

Yet one more possibility to introduce monopoles into the electroweak theory was found by Cho and Maison (CM) [19], who used the same form for the Higgs field as for the Nambu monopole (1.2), but assumed that its singularity at $\vartheta = \pi$ is a gauge artefact and can be handled by using two local gauges, as for the Dirac monopole. In other words, one assumes that $\Phi_{\rm mon}$ in (1.2) should be used only in the upper hemisphere where it is regular, while in the lower hemisphere one uses its gauge-transformed version $\tilde{\Phi}_{\rm mon} = e^{i\varphi}\Phi_{\rm mon}$ which is regular for $\vartheta \to \pi$. The U(1) gauge transformation $e^{i\varphi}$ relating the two gauges is regular in the equatorial transition region. This provides a globally regular description for a static and spherically symmetric monopole whose magnetic charge is the same as for the Dirac monopole (1.1) with $n = 2$.

The CM monopole solution contains a regular non-Abelian part which is similar to the t'Hooft-Polyakov monopole, but it contains also a Coulombian U(1) hypercharge field which diverges at the origin thus rendering the energy infinite [19]. The latter feature is not very appealing and there have been attempts to regularize the monopole energy in some way, but they require to modify the Lagrangian of the theory [20–24]. At the same time, since the Standard Model describes the real world extremely well, it seems to be more logical to consider the CM monopole as it is, with infinite energy. In any case, its energy certainly becomes finite when gravity is taken into account [25].

In a recent analysis, the stability of the CM monopole was studied and it was found that it is stable with respect to arbitrary (small) perturbations [26]. At the same time, all Dirac monopoles with $|n| > 1$ are unstable with respect to perturbations in the sector with the angular momentum $j = |n|/2 - 1$. In particular, the Dirac monopole with $|n| = 2$ is unstable

only in the $j = 0$ sector while the CM monopole is stable and also has $|n| = 2$. This suggests that the CM monopole may be viewed as a stable remnant of the decay of the Abelian monopole. One may similarly conjecture that stable remnants exist also for monopoles with $|n| > 2$, hence the CM monopole is just the first member of a sequence of non-Abelian monopole solutions labeled by their magnetic charge n. Only the CM monopole is spherically symmetric, while the non-Abelian monopoles with $|n| > 2$ are not rotationally invariant.

In what follows, we confirm this conjecture by explicitly constructing generalizations of the Cho-Maison monopole for higher values of the magnetic charge in the simplest case of axial symmetry. At the same time, we could not yet check their stability. We construct the solutions numerically for various values of the charge, compute their regularized energy, the quadrupole momentum, and study their inner structure. It turns out that the elementary Cho-Maison monopoles inside the multi-charge monopole merge together to form a magnetically charged toroidal condensate, accompanied by circular electric currents.

Monopoles have zero dipole moment but a finite quadrupole momentum that rapidly increases with growing magnetic charge. For large values of the charge, the monopoles are strongly squashed and develop in the center a bubble of symmetric phase containing the U(1) hypercharge field created by a pointlike magnetic charge at the center. This field is strong enough to suppress all other fields and restore the full electroweak gauge symmetry in the bubble. The bubble is encircled by a belt of broken phase containing the W-condensate in the form of a magnetically charged ring squeezed between two superconducting rings of oppositely directed electric currents. The total magnetic charge of the monopole splits into the pointlike U(1) part at the origin and the SU(2) part smoothly distributed over the ring volume. The pointlike charge at the origin makes an infinite contribution to the energy, but the energy is expected to become finite after taking gravity into account, which will provide a cutoff via creating an event horizon to shield the U(1) charge.

We use the same ansatz for the axially symmetric fields as the one previously employed to construct the electroweak sphalerons [27, 28]. The sphalerons are static and spherically symmetric if $\theta_{\rm w} = 0$ [29, 30], while for $\theta_{\rm w} \neq 0$ they are axially symmetric [27, 28, 31]. Sphalerons are quite different physically from monopoles – they are neutral and unstable [32], but from the technical viewpoint they are similar to monopoles, and we were able to obtain solutions of both types by simply changing the boundary conditions in the equations. This provides a good consistency check for our numerical scheme. Besides, sphalerons contain inside monopoles and antimonopoles of Nambu [33], and we find that these Nambu monopoles and our monopoles, after subtracting their divergent U(1) part, are very similar to each other –

they have the same quantization condition for the magnetic charge, a similar ring distribution of the charge for $|n| > 2$, and almost the same energy for $|n| = 2$.

The rest of the text is organized as follows. Equations of the classical electroweak theory are presented in Section II, and the axially symmetric fields are described in Section III. This section also shows the desingularization procedure for removing the line singularities in the fields. The spherically symmetric monopole and sphaleron are described in Section V. The main results – the non-Abelian multi-monopole solutions and their various properties – are presented in Section V. The comparison with the sphalerons is discussed in Section VI, and concluding remarks are given in Section VII. The two Appendices contain technical details, such as solutions in the asymptotic region, solutions close to the origin, and properties of the gauge conditions.

In our analysis we used the FreeFem++ numerical solver based on the finite element method [34]. Each of us run his own numerical code and we compared our results till reaching the agreement.

II. ELECTROWEAK THEORY

The dimensionful action of the bosonic part of the electroweak theory of Weinberg and Salam (WS) can be represented in the form

$$\mathbf{S} = \frac{1}{\boldsymbol{c}\,\boldsymbol{g}_0^2} \int \mathcal{L}_{\rm WS} \sqrt{-\mathrm{g}}\, d^4x \,, \tag{2.1}$$

with the Lagrangian

$$\mathcal{L}_{\rm WS} = -\frac{1}{4g^2}\, \mathrm{W}^a_{\mu\nu} \mathrm{W}^{a\mu\nu} - \frac{1}{4g'^2}\, B_{\mu\nu} B^{\mu\nu} - (D_\mu \Phi)^\dagger D^\mu \Phi - \frac{\beta}{8} \left(\Phi^\dagger \Phi - 1\right)^2 , \tag{2.2}$$

where all fields and couplings as well as the spacetime coordinates x^μ and metric $\mathrm{g}_{\mu\nu}$ are rendered dimensionless by rescaling. The Abelian U(1) and non-Abelian SU(2) field strengths are

$$B_{\mu\nu} = \partial_\mu B_\nu - \partial_\nu B_\mu \,, \qquad \mathrm{W}^a_{\mu\nu} = \partial_\mu \mathrm{W}^a_\nu - \partial_\nu \mathrm{W}^a_\mu + \epsilon_{abc} \mathrm{W}^b_\mu \mathrm{W}^c_\nu \,, \tag{2.3}$$

while the Higgs field Φ is in the fundamental representation of SU(2) with the covariant derivative

$$D_\mu \Phi = \left(\partial_\mu - \frac{i}{2}\, B_\mu - \frac{i}{2}\, \tau^a \mathrm{W}^a_\mu \right) \Phi \,, \tag{2.4}$$

where τ^a are the Pauli matrices. The two coupling constants are $g = \cos\theta_{\rm w}$ and $g' = \sin\theta_{\rm w}$ where the physical value of the Weinberg angle is such that $g'^2 = \sin^2\theta_{\rm w} = 0.23$.

The dimensionful parameters (we denote all dimensionful quantities boldfaced) in the action (2.1) are the speed of light $\boldsymbol{c}$ and also $\boldsymbol{g}_0$ related to the electron charge $\boldsymbol{e}$,

$$\frac{\boldsymbol{e}^2}{4\pi\boldsymbol{\hbar c}} = \frac{\boldsymbol{\hbar c}}{4\pi}\left(g g' \boldsymbol{g}_0\right)^2 \approx \frac{1}{137} \qquad \Rightarrow \qquad \boldsymbol{e} = \boldsymbol{\hbar c g}_0 e \qquad \text{with} \qquad e \equiv g g' \,. \tag{2.5}$$

The dimensionful fields often used in the literature are $\boldsymbol{B}_\mu = (\boldsymbol{\Phi}_0/g')B_\mu$, $\boldsymbol{W}^a_\mu = (\boldsymbol{\Phi}_0/g)\mathrm{W}^a_\mu$ and $\boldsymbol{\Phi} = \boldsymbol{\Phi}_0\Phi$ where $\boldsymbol{\Phi}_0 = 246$ GeV is the Higgs field vacuum expectation value. The dimensionful coordinates are $\boldsymbol{x}^\mu = \boldsymbol{L}_{\rm WS}\, x^\mu$ with the electroweak length scale $\boldsymbol{L}_{\rm WS} = 1/(\boldsymbol{g}_0\boldsymbol{\Phi}_0) = 1.52 \times 10^{-16}$ cm.

The theory is invariant under SU(2)×U(1) gauge transformations

$$\Phi \to \mathrm{U}\Phi, \qquad \mathcal{W} \to \mathrm{U}\mathcal{W}\mathrm{U}^{-1} + i\mathrm{U}\partial_\mu \mathrm{U}^{-1} dx^\mu \,, \tag{2.6}$$

with

$$\mathcal{W} = \frac{1}{2}\left(B_\mu + \tau^a \mathrm{W}^a_\mu\right) dx^\mu \,, \qquad \mathrm{U} = \exp\left(\frac{i}{2}\,\Sigma + \frac{i}{2}\,\tau^a\theta^a\right), \tag{2.7}$$

where Σ and θ^a are functions of x^μ. Varying the action gives the equations,

$$\begin{aligned}
\nabla^\mu B_{\mu\nu} &= g'^2\,\frac{i}{2}\left(\Phi^\dagger D_\nu\Phi - (D_\nu\Phi)^\dagger\Phi\right) \equiv g'^2 J_\nu, \\
\mathcal{D}^\mu \mathrm{W}^a_{\mu\nu} &= g^2\,\frac{i}{2}\left(\Phi^\dagger\tau^a D_\nu\Phi - (D_\nu\Phi)^\dagger\tau^a\Phi\right) \equiv g^2 J^a_\nu, \\
D_\mu D^\mu\Phi &- \frac{\beta}{4}\left(\Phi^\dagger\Phi - 1\right)\Phi = 0,
\end{aligned} \tag{2.8}$$

with $\mathcal{D}_\mu \mathrm{W}^a_{\alpha\beta} = \nabla_\mu \mathrm{W}^a_{\alpha\beta} + \epsilon_{abc}\mathrm{W}^b_\mu \mathrm{W}^c_{\alpha\beta}$ where ∇_μ is the geometrical covariant derivative with respect to the spacetime metric. Varying the action with respect to the latter determines the energy-momentum tensor,

$$T_{\mu\nu} = \frac{1}{g^2}\,\mathrm{W}^a{}_{\mu\sigma}\mathrm{W}^a{}_\nu{}^\sigma + \frac{1}{g'^2} B_{\mu\sigma}B_\nu{}^\sigma + (D_\mu\Phi)^\dagger D_\nu\Phi + (D_\nu\Phi)^\dagger D_\mu\Phi + g_{\mu\nu}\mathcal{L}_{\rm WS} \,. \tag{2.9}$$

The vacuum is defined as the configuration with $T_{\mu\nu} = 0$. Modulo gauge transformations, it can be chosen as

$$\mathrm{W}^a_\mu = B_\mu = 0, \qquad \Phi = \begin{pmatrix} 0 \\ 1 \end{pmatrix}. \tag{2.10}$$

Allowing for small fluctuations around the vacuum and linearizing the field equations with respect to the fluctuations gives the perturbative mass spectrum containing the massless photon and the massive Z, W and Higgs bosons with dimensionless masses

$$m_{\rm Z} = \frac{1}{\sqrt{2}}, \qquad m_{\rm W} = g\, m_{\rm Z}, \qquad m_{\rm H} = \sqrt{\beta}\, m_{\rm Z}. \tag{2.11}$$

Multiplying these by $\boldsymbol{e\Phi}_0/(gg')$ gives the dimensionful masses, for example one has $\boldsymbol{m}_{\rm Z}\boldsymbol{c}^2 = \boldsymbol{e\Phi}_0/(\sqrt{2}gg') \approx 91$ GeV. Using the Higgs mass $\boldsymbol{m}_{\rm H}\boldsymbol{c}^2 \approx 125$ GeV yields the value $\beta \approx 1.88$.

Summarizing, the dimensionless parameters in the equations are

$$g'^2 = 0.23, \qquad g^2 = 1 - g'^2, \qquad \beta = 1.88. \tag{2.12}$$

We shall adopt the definition of Nambu for the electromagnetic and Z fields [15],

$$F_{\mu\nu} = \frac{g}{g'}\, B_{\mu\nu} - \frac{g'}{g}\, N^a \mathrm{W}^a_{\mu\nu}\,, \qquad Z_{\mu\nu} = B_{\mu\nu} + N^a \mathrm{W}^a_{\mu\nu}\,, \tag{2.13}$$

where $N^a = \Phi^\dagger \tau^a \Phi/(\Phi^\dagger\Phi)$. The magnetic part of $F_{\mu\nu}$ will be denoted by the calligraphic symbol, $\mathcal{B}^i = \frac{1}{2}\epsilon^{ijk}F_{jk}$, not to be confused with the hypercharge field $B = B_\mu dx^\mu$.

Using the electromagnetic tensors $F_{\mu\nu}$ and its dual,

$$\tilde{F}^{\mu\nu} = \frac{1}{2\sqrt{-\mathrm{g}}}\,\epsilon^{\mu\nu\alpha\beta}F_{\alpha\beta}\,, \tag{2.14}$$

one can define the conserved electric and magnetic currents,

$$J^\mu = \frac{1}{4\pi}\,\frac{1}{\sqrt{-\mathrm{g}}}\,\partial_\nu\left(\sqrt{-\mathrm{g}}\,F^{\mu\nu}\right), \qquad \tilde{J}^\mu = \frac{1}{4\pi}\,\frac{1}{\sqrt{-\mathrm{g}}}\,\partial_\nu\left(\sqrt{-\mathrm{g}}\,\tilde{F}^{\mu\nu}\right). \tag{2.15}$$

Since $F_{\mu\nu}$ consists of two parts, both J^μ and $\tilde{J}^\mu$ split into a sum of two separately conserved currents – the U(1) current determined by the contribution of $B_{\mu\nu}$ and the SU(2) current determined by $W^a_{\mu\nu}$. We shall be considering purely magnetic systems for which the non-vanishing components are the electric current J^k and the magnetic charge density $\tilde{J}^0$. The magnetic charge and its density then split into the U(1) and SU(2) parts,

$$\tilde{J}^0 = \frac{1}{4\pi}\,\vec{\nabla}\cdot\vec{\mathcal{B}} \equiv \rho_{\mathrm{U}(1)} + \rho_{\mathrm{SU}(2)}\,, \tag{2.16}$$

and

$$P = \int\left(\rho_{\mathrm{U}(1)} + \rho_{\mathrm{SU}(2)}\right)\sqrt{-g}\,d^3x \equiv P_{\mathrm{U}(1)} + P_{\mathrm{SU}(2)}, \tag{2.17}$$

where $P_{\mathrm{U}(1)}$ and $P_{\mathrm{SU}(2)}$ are separately conserved. Since the B field is Abelian, one has

$$P_{\mathrm{U}(1)} = \frac{g}{g'}\,\frac{1}{4\pi}\oint_{S^2} dB\,, \tag{2.18}$$

where the integration is performed over a two-sphere at infinity. This integral vanishes unless B is topologically non-trivial, in which case the value of the integral is determined by the topology and does not depend on the radius of the sphere.

III. AXIAL SYMMETRY

To describe axially symmetric fields, it is convenient to express the spacetime metric in spherical coordinates,

$$\mathrm{g}_{\mu\nu}dx^\mu dx^\nu = -dt^2 + dr^2 + r^2\left(d\vartheta^2 + \sin^2\vartheta d\varphi^2\right). \tag{3.1}$$

Let $\mathrm{T}_a = \frac{1}{2}\tau_a$ be the SU(2) gauge group generators such that $[\mathrm{T}_a, \mathrm{T}_b] = i\epsilon_{abc}\mathrm{T}_c$. The SU(2) gauge field, the U(1) hypercharge field and the Higgs field are

$$\begin{aligned} W \equiv \mathrm{T}_a \mathrm{W}^a_\mu dx^\mu &= \mathrm{T}_2\left(F_1\, dr + F_2\, d\vartheta\right) + \nu\left(\mathrm{T}_3\, F_3 - \mathrm{T}_1 F_4\right) d\varphi\,, \\ B \equiv B_\mu dx^\mu &= \nu\, Y\, d\varphi\,, \qquad \Phi = \begin{pmatrix}\phi_1\\ \phi_2\end{pmatrix}, \end{aligned} \tag{3.2}$$

where $F_1, F_2, F_3, F_4, Y, \phi_1, \phi_2$ are 7 real-valued functions of r, ϑ and ν is a real parameter. The SU(2) field here corresponds to the purely magnetic ansatz of Rebbi and Rossi [35]. The ansatz keeps its form under gauge transformations (2.6) generated by $\mathrm{U} = \exp\{i\chi(r,\vartheta)\mathrm{T}_2\}$, whose effect is

$$\begin{aligned} F_1 &\to F_1 + \partial_r\chi, \qquad F_2 \to F_2 + \partial_\vartheta\chi, \qquad Y \to Y, \\ F_3 &\to F_3\cos\chi - F_4\sin\chi\,, \qquad F_4 \to F_4\cos\chi + F_3\sin\chi\,, \\ \phi_1 &\to \phi_1\cos(\chi/2) + \phi_2\sin(\chi/2), \qquad \phi_2 \to \phi_2\cos(\chi/2) - \phi_1\sin(\chi/2). \end{aligned} \tag{3.3}$$

Inserting this to (2.9) defines the energy,

$$E = \int T_{00}\sqrt{-\mathrm{g}}\, d^3x = 2\pi\int_0^\infty dr\int_0^\pi d\vartheta\left(\frac{\mathcal{E}_W}{2g^2} + \frac{\mathcal{E}_B}{2g'^2} + \mathcal{E}_\Phi + V\right), \tag{3.4}$$

where

$$\begin{aligned} \mathcal{E}_W &= \left(\partial_\vartheta F_1 - \partial_r F_2\right)^2\sin\vartheta \\ &\quad + \left(\left(\partial_r F_3 + F_1F_4\right)^2 + \left(\partial_r F_4 - F_1F_3\right)^2\right)\frac{\nu^2}{\sin\vartheta} \\ &\quad + \left(\left(\partial_\vartheta F_3 + F_2F_4\right)^2 + \left(\partial_\vartheta F_4 - F_2F_3\right)^2\right)\frac{\nu^2}{r^2\sin\vartheta}\,, \\ \mathcal{E}_B &= \left(\left(\partial_r Y\right)^2 + \frac{1}{r^2}\left(\partial_\vartheta Y\right)^2\right)\frac{\nu^2}{\sin\vartheta}\,, \\ \mathcal{E}_\Phi &= r^2\left(\left(\partial_r\phi_1 - \frac{F_1}{2}\,\phi_2\right)^2 + \left(\partial_r\phi_2 + \frac{F_1}{2}\,\phi_1\right)^2\right)\sin\vartheta \\ &\quad + \left(\left(\partial_\vartheta\phi_1 - \frac{F_2}{2}\,\phi_2\right)^2 + \left(\partial_\vartheta\phi_2 + \frac{F_2}{2}\,\phi_1\right)^2\right)\sin\vartheta \\ &\quad + \left(\left((F_3+Y)\phi_1 - F_4\phi_2\right)^2 + \left((F_3-Y)\phi_2 + F_4\phi_1\right)^2\right)\frac{\nu^2}{4\sin\vartheta}\,, \\ V &= \frac{\beta r^2}{8}\left(\phi_1^2 + \phi_2^2 - 1\right)^2\sin\vartheta\,. \end{aligned} \tag{3.5}$$

The energy is gauge invariant. Modulo gauge transformations (3.3), the zero energy configuration is

$$F_1 = F_2 = F_4 = \phi_1 = 0, \quad \phi_2 = 1, \qquad F_3 = Y = const. \equiv Y_\infty. \tag{3.6}$$

This vacuum keeps its form under gauge transformations generated by $\mathrm{U} = \exp\{i\,\mathcal{C}\,\nu\varphi(1+\tau_3)/2\}$ with a constant $\mathcal{C}$, whose effect is $Y_\infty \to Y_\infty + \mathcal{C}$.

The above formulas apply to describe both monopoles and sphalerons. The difference between the two cases is in the boundary conditions for the field amplitudes. Specifically, let us require the energy to be invariant under the reflection in the equatorial plane, $\vartheta \to \pi - \vartheta$. This implies that certain fields amplitudes do not change so that they are "even" while the others change sign under the reflection hence they are "odd". Assuming that $\phi_2 \to 1$ at infinity, the direct inspection of Eqs.(3.4),(3.5) shows two possible options that we call "monopole case" and "sphaleron case":

$$\begin{aligned} &\underline{\text{monopole case:}} \ \text{ odd } \ F_1, F_3, Y, \phi_1 \ \text{ and even } \ F_2, F_4, \phi_2; \\ &\underline{\text{sphaleron case:}} \ \text{ odd } \ F_1, F_4, \phi_1 \ \text{ and even } \ F_2, F_3, Y, \phi_2. \end{aligned} \tag{3.7}$$

Let us redefine the gauge field amplitudes as follows,

$$\begin{aligned} F_1 = -\frac{H_1(r,\vartheta)}{r}, \quad F_2 = H_2(r,\vartheta), \quad F_3 = \Theta(\vartheta) + H_3(r,\vartheta)\sin\vartheta\,, \\ F_4 = H_4(r,\vartheta)\sin\vartheta\,, \qquad Y = \Theta(\vartheta) + y(r,\vartheta)\sin\vartheta\,, \end{aligned} \tag{3.8}$$

where the function $\Theta(\vartheta)$ and the behaviour under $\vartheta \to \pi - \vartheta$ are as follows:

$$\begin{aligned} &\underline{\text{monopole case:}} \quad \Theta(\vartheta) = \cos\vartheta, \qquad \text{odd } \ H_1, H_3, y, \phi_1 \ \text{ and even } \ H_2, H_4, \phi_2; \\ &\underline{\text{sphaleron case:}} \quad \Theta(\vartheta) = 1, \qquad \text{odd } \ H_1, H_4, \phi_1 \ \text{ and even } \ H_2, H_3, y, \phi_2\,. \end{aligned} \tag{3.9}$$

The energy density will be finite at the polar axis if only all coefficients in front of the $1/\sin\vartheta$ terms in (3.5) vanish, which requires that

$$H_1 = H_3 = y = \phi_1 = 0, \qquad H_2 = H_4 \qquad \text{for} \qquad \vartheta = 0, \pi. \tag{3.10}$$

These conditions guarantee that the fields can be transformed to a regular gauge. Specifically, the φ-components of the gauge fields in (3.2) do not vanish for $\vartheta = 0, \pi$, which implies a line singularity of the Dirac string type along the symmetry axis. However, this singularity can be gauged away, but if only the parameter ν in (3.2) is integer. The regularizing gauge transformation for monopoles is not the same as for sphalerons.

A. Removing string singularity in the monopole case

Setting $\Theta(\vartheta) = \cos\vartheta$ in (3.8), the gauge transformation that removes the singularity in (3.2) is generated by

$$\mathrm{U}_\pm = e^{-i\nu\varphi \mathrm{T}_3} e^{-i\vartheta \mathrm{T}_2} e^{\pm i\nu\varphi/2} = e^{\pm i\nu\varphi/2} \begin{pmatrix} \cos\frac{\vartheta}{2}\, e^{-i\nu\varphi/2} & -\sin\frac{\vartheta}{2}\, e^{-i\nu\varphi/2} \\ \sin\frac{\vartheta}{2}\, e^{i\nu\varphi/2} & \cos\frac{\vartheta}{2}\, e^{i\nu\varphi/2} \end{pmatrix}, \tag{3.11}$$

which brings the SU(2) field to the form

$$W = \mathrm{T}_\varphi \left(-\frac{H_1}{r}\, dr + (H_2 - 1)\, d\vartheta \right) + \nu \left(\mathrm{T}_r\, H_3 + \mathrm{T}_\vartheta\, (1 - H_4) \right) \sin\vartheta\, d\varphi\,. \tag{3.12}$$

This form of the field (and the notation) is often used in the literature; see, e.g., [36]. Here the angle-dependent generators,

$$\mathrm{T}_r = n^a \mathrm{T}_a, \qquad \mathrm{T}_\vartheta = \partial_\vartheta \mathrm{T}_r, \qquad \mathrm{T}_\varphi = \frac{1}{\nu \sin\vartheta}\, \partial_\varphi \mathrm{T}_r, \tag{3.13}$$

are expressed in terms of the unit vector

$$n^a = [\sin\vartheta\cos(\nu\varphi), \sin\vartheta\sin(\nu\varphi), \cos\vartheta\,]\,. \tag{3.14}$$

They satisfy the standard commutation relations, for example $[\mathrm{T}_r, \mathrm{T}_\vartheta] = i\mathrm{T}_\varphi$. It is clear that the parameter ν should be integer since otherwise the vector n^a is not single-valued. Now, (3.10) implies that in the vicinity of the symmetry axis $W = (\mathrm{T}_1\, dx^2 - \mathrm{T}_2\, dx^1)(1 - H_2) + \ldots$ where $x^a = r n^a$ are the Cartesian coordinates and the dots denote terms that vanish at the axis. This field is regular at the axis and the Dirac string is gone.

The "+" and "−" sign choices in (3.11) determine two locally regular gauges for B, Φ:

$$B_\pm = \nu\,(\cos\vartheta \pm 1 + y\, \sin\vartheta)\, d\varphi\,, \quad \Phi_\pm = e^{\pm i\nu\varphi/2} \begin{pmatrix} (\,\phi_1\, \cos\frac{\vartheta}{2} - \phi_2\, \sin\frac{\vartheta}{2}\,)\, e^{-i\nu\varphi/2} \\ (\,\phi_1\, \sin\frac{\vartheta}{2} + \phi_2\, \cos\frac{\vartheta}{2}\,)\, e^{+i\nu\varphi/2} \end{pmatrix}. \tag{3.15}$$

Here B_- and Φ_- are regular for $\vartheta = 0$, but B_- shows the Dirac string singularity along the negative z-axis at $\vartheta = \pi$, whereas Φ_- has no limit there. Therefore, this gauge can be used only in the upper part of the sphere, for $\vartheta \in [0, \pi - \epsilon)$. On the other hand, B_+ and Φ_+ are regular for $\vartheta = \pi$ and can be used in the lower hemisphere, for $\vartheta \in (\epsilon, \pi]$. Therefore, B and Φ will be completely regular if one uses two local gauges: B_-, Φ_- in the upper hemisphere and B_+, Φ_+ in the lower hemisphere. The transition from one local gauge to the other is performed in the equatorial region, $\epsilon < \vartheta < \pi - \epsilon$, and provided by $\mathrm{U} = \exp(i\nu\varphi)$, which is single-valued if $\nu \in \mathbb{Z}$. This provides a regular description for all fields.

The U(1) part of the magnetic charge in (2.18) is defined by the integral

$$\frac{1}{4\pi} \oint_{S^2} dB = \frac{1}{4\pi} \oint_{S^1} (B_- - B_+) = -\frac{\nu}{2\pi} \oint_{S^1} d\varphi = -\nu\,, \tag{3.16}$$

where S^1 is a circle around the equatorial region of S^2 where both B_+ and B_- are regular. The winding number ν is the topological index – the first Chern class of the U(1) bundle over S^2. The U(1) part of the magnetic charge and the corresponding charge density are

$$P_{\mathrm{U}(1)} = -\frac{g}{g'}\,\nu\,, \qquad \rho_{\mathrm{U}(1)} = P_{\mathrm{U}(1)}\delta^3(\vec{x}), \tag{3.17}$$

so that the charge is pointlike and located at the origin.

B. Removing string singularity in the sphaleron case

Setting $\Theta(\vartheta) = 1$ in (3.8), the gauge transformation that removes the singularity in (3.2) is generated by $\mathrm{U} = \exp\{-i\nu(1+\tau_3)\,\varphi/2\}$. This brings the fields to the form

$$\begin{aligned} W &= \mathrm{T}_\varphi\left(-\frac{H_1}{r}\,dr + H_2\,d\vartheta\right) + \nu\,(\mathrm{T}_3\,H_3 - \mathrm{T}_\rho\,H_4)\sin\vartheta\,d\varphi\,, \\ B &= \nu\,y\,\sin\vartheta\,d\varphi\,, \qquad\qquad \Phi = \begin{pmatrix} e^{-i\nu\varphi}\,\phi_1 \\ \phi_2 \end{pmatrix}, \end{aligned} \tag{3.18}$$

where $\mathrm{T}_\rho = \cos(\nu\varphi)\mathrm{T}_1 + \sin(\nu\varphi)\mathrm{T}_2$. Here B and Φ are regular at the symmetry axis and one has close to the axis $W = (\mathrm{T}_1\,dx^2 - \mathrm{T}_2\,dx^1)H_2 + \ldots$ which is also regular.

Defining $\tilde{H}_2 = 1 + H_2$, $\tilde{H}_3 = H_3\,\cos\vartheta - H_4\,\sin\vartheta$, $\tilde{H}_1 = 1 + H_3\,\sin\vartheta + H_4\,\cos\vartheta$, the field W in (3.18) can be represented exactly in the same form as W in (3.12),

$$W = \mathrm{T}_\varphi\left(-\frac{H_1}{r}\,dr + (\tilde{H}_2 - 1)\,d\vartheta\right) + \nu\left(\mathrm{T}_r\,\tilde{H}_3 + \mathrm{T}_\vartheta\,(1-\tilde{H}_4)\right)\sin\vartheta\,d\varphi\,, \tag{3.19}$$

which form is often used in the literature [37–39]. This does not mean that sphalerons and monopoles can be related by simply redefining the field amplitudes, since the fields B, Φ in the monopole case given by (3.15) are not the same as those in in the sphaleron case given by (3.18).

The B field in the sphaleron case case is topologically trivial, hence the U(1) magnetic charge density vanishes. The SU(2) part of the charge density, $\rho_{\mathrm{SU}(2)}$, does not necessarily vanish, but the total magnetic charge is zero, as we shall see below.

Summarizing, the fields (3.2) can be transformed to a regular gauge only if ν is integer. This is an important conclusion, since the field equations can formally be considered for any real ν giving perfectly smooth solutions for the 7 field amplitudes $H_1, \ldots, \phi_2$. However, unless ν is integer, the fields will contain unremovable string singularities along the symmetry axis. The only exception is the special case when $H_1 = H_2 = H_3 = H_4 = 0$ when the SU(2) field becomes Abelian. As will be shown below, ν can then assume also half-integer values.

C. Fixing the gauge

The field equations can be obtained by injecting (3.8) to the energy (3.4) and varying with respect to $H_1, H_2, H_3, H_4, y, \phi_1, \phi_2$. These equations admit pure gauge solutions due to the residual gauge invariance (3.3), and such zero modes should be removed by fixing the gauge, since otherwise the differential operators in the equations will not be invertible. The gauge can be fixed setting to zero the divergence of the two-vector $F_1\, dr + F_2\, d\vartheta$ in (3.2), which requires that [27, 28]

$$r\partial_r H_1 = \partial_\vartheta H_2. \tag{3.20}$$

The advantage of this gauge condition is that it is simple, globally defined and yields a good numerical convergence. The disadvantage, as will be shown in Appendix A, is that it gives rise to a spurious long-range mode contained in solutions at large r. This spurious mode can be removed by passing to the unitary gauge, but the latter turns out to be singular at the origin, as will be shown in Appendix B. Therefore, the gauge condition (3.20) seems to be preferable.

Using this condition, all equations assume a manifestly elliptic form with the standard differential operator

$$\Delta = \partial_{rr}^2 + \frac{2}{r}\,\partial_r + \frac{1}{r^2}\left(\partial_{\vartheta\vartheta}^2 + \cot\vartheta\,\partial_\vartheta\right). \tag{3.21}$$

The equations should be solved in the domain $r \in [0, \infty)$, $\vartheta \in [0, \pi/2]$, and it is also convenient to use the compact radial variable $x \in [0, 1]$ related to r via

$$r = \frac{x}{1-x}. \tag{3.22}$$

The boundary conditions at $\vartheta = 0, \pi/2$ have been described above, while those at the origin $r = 0$ and at infinity $r = \infty$ will be described below.

IV. SPHERICALLY SYMMETRIC SOLUTIONS

Solutions of the field equations can be spherically symmetric in exceptional cases, and such solutions can be magnetically charged (monopoles) or neutral (sphalerons).

A. Monopoles

Choosing in (3.8)

$$\Theta(\vartheta) = \cos\vartheta, \qquad H_1 = H_3 = y = \phi_1 = 0, \qquad H_2 = H_4 = f(r), \qquad \phi_2 = \phi(r), \tag{4.1}$$

the angular variables decouple and the equations reduce to

$$\begin{aligned} f'' &= \nu^2\,\frac{f(f^2-1)}{r^2} + \frac{g^2}{2}\,\phi^2 f\,, \\ (r^2\phi')' &= \frac{1}{4}\,(\nu^2+1)f^2\phi + \frac{\beta r^2}{4}\,(\phi^2-1)\phi\,, \\ (\nu^2-1)f' &= (\nu^2-1)f\phi = 0. \end{aligned} \tag{4.2}$$

1. *Abelian monopoles of Dirac*

The simplest solution of these equations exists for any value of ν,

$$f = 0, \qquad \phi = 1. \tag{4.3}$$

This describes the Dirac magnetic monopole embedded into the electroweak theory. Returning for a moment to the original parameterization (3.2) yields

$$B = \nu\cos\vartheta\,d\varphi, \qquad W = T_3\,B, \qquad \Phi = \begin{pmatrix} 0 \\ 1 \end{pmatrix}, \tag{4.4}$$

and after the gauge transformation generated by $\mathrm{U}_\pm = \exp\left(\pm i\nu\varphi(1+\tau_3)/2\right)$ this becomes

$$B_\pm = \nu(\cos\vartheta \pm 1)\,d\varphi, \qquad W_\pm = T_3\,B_\pm, \qquad \Phi = \begin{pmatrix} 0 \\ 1 \end{pmatrix}. \tag{4.5}$$

Here W_-, B_- are regular at $\vartheta = 0$ and can be used in the northern hemisphere, while W_+, B_+ are regular at $\vartheta = \pi$ and can be used in the southern hemisphere. Using these two local gauges provides a completely regular description. The transition from W_-, B_- to W_+, B_+ is provided by the gauge transformation in the equatorial region with

$$\mathrm{U} = \exp\left(i\nu\,\varphi(1+\tau_3)\right) = \begin{pmatrix} \exp\left(2i\,\nu\varphi\right) & 0 \\ 0 & 1 \end{pmatrix}, \tag{4.6}$$

which is single-valued if ν is integer or *half-integer*. The latter is an important conclusion since generically ν should be integer, but we see that half-integer values of ν are also allowed in the particular case when the field configuration is Abelian.

Computing the electromagnetic field $F_{\mu\nu}$ in (2.13) shows that it admits a potential, $F = d\mathcal{A}$ with

$$\mathcal{A} = \mathcal{A}_\mu dx^\mu = \left(\frac{g}{g'}\,B_\mu + \frac{g'}{g}\,W^3_\mu\right)dx^\mu = \frac{g^2+g'^2}{gg'}B_\pm = \frac{\nu}{e}\,(\cos\vartheta \pm 1)\,d\varphi\,, \tag{4.7}$$

which is the potential of the Dirac monopole

$$\vec{\mathcal{B}} = \vec{\nabla}\wedge\vec{\mathcal{A}} = \frac{P\,\vec{r}}{r^3}\,, \tag{4.8}$$

with the magnetic charge

$$P = -\frac{\nu}{e}\,. \tag{4.9}$$

Here $e = gg'$ is the dimensionless electron charge defined in (2.5). It will be commonly assumed below that $\nu > 1$, hence the magnetic charge P defined by (4.9) is *negative* (the opposite sign convention for the charge was made in [26]). Since ν in (4.9) can be integer or half-integer, it follows that

$$n \equiv -2\nu \tag{4.10}$$

is integer (notice the minus sign here), hence the magnetic charge fulfills the standard Dirac quantization condition,

$$eP = \frac{n}{2} \qquad \text{with} \qquad n \in \mathbb{Z}. \tag{4.11}$$

The magnetic charge can be split into two parts according to (2.17), corresponding to the Abelian B_μ and non-Abelian W^3_μ contributions to (4.7),

$$P = P_{\mathrm{U}(1)} + P_{\mathrm{SU}(2)} \qquad \text{with} \qquad P_{\mathrm{U}(1)} = g^2 P\,, \quad P_{\mathrm{SU}(2)} = g'^2 P\,, \tag{4.12}$$

and it is worth noting that the non-Abelian part,

$$P_{\mathrm{SU}(2)} = \sin^2\theta_{\mathrm{w}} \times \frac{n}{2e} = \frac{g'}{g}\,\frac{n}{2}, \tag{4.13}$$

is quantized as in the Nambu formula (1.3). The U(1) and SU(2) parts of the magnetic charge density (2.16) are

$$\rho_{\mathrm{U}(1)} = g^2 P \delta^3(\vec{x}), \qquad \rho_{\mathrm{SU}(2)} = g'^2 P \delta^3(\vec{x}). \tag{4.14}$$

Both parts of the magnetic charge make singular contributions to the energy

$$E = \frac{2\pi\nu^2}{g'^2}\int_0^\infty \frac{dr}{r^2} + \frac{2\pi\nu^2}{g^2}\int_0^\infty \frac{dr}{r^2} \equiv E_{\mathrm{U}(1)} + E_{\mathrm{SU}(2)}. \tag{4.15}$$

Summarizing, the Dirac monopole can be viewed as a superposition of two pointlike magnetic charges $P_{\mathrm{U}(1)}$ and $P_{\mathrm{SU}(2)}$ located at the origin, both making an infinite contribution to the energy. Below we shall be considering other, more general solutions approaching the Dirac monopole configuration in the far field region. Their $P_{\mathrm{U}(1)}$ charge is still pointlike, but the $P_{\mathrm{SU}(2)}$ charge is smoothly distributed over a finite volume and its contribution to the total energy is finite. The simplest solution of this type is the Cho-Maison monopole.

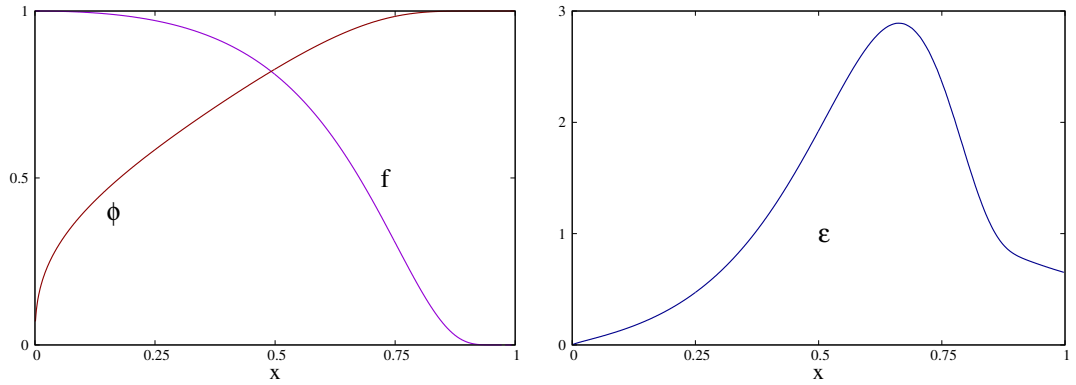


FIG. 1. Profiles of the gauge field and Higgs amplitudes f and ϕ (left) and the energy density (right) against the compact radial coordinate x for the spherically symmetric CM monopole with $g'^2 = 0.23$.

2. *The non-Abelian monopole of Cho and Maison*

For $\nu = \pm 1$ (hence for $n = \pm 2$), Eqs.(4.2) admit a smooth non-Abelian solution for which the amplitudes f, ϕ interpolate between the following asymptotic values: $f = 1 + \mathcal{O}(r^2)$, $\phi = \mathcal{O}(r^\delta)$ for $r \to 0$, where $\delta = (\sqrt{3} - 1)/2$, and $f = \mathcal{O}\left(e^{-m_W r}\right)$, $\phi = 1 + \mathcal{O}\left(e^{-m_H r}\right)$ for $r \to \infty$; see Fig.1. This solution was found numerically by Cho and Maison (CM) [19], and its existence was proven by Yang [40]. At infinity the fields approach those for the Dirac monopole with $n = \pm 2$, while at the origin the non-Abelian field is regular and its contribution to the energy is finite. However, the U(1) contribution to the energy is still infinite due to the $\mathcal{E}_B$ term in (3.5), since for $Y = \cos\vartheta$ and $\nu = \pm 1$ one has $\mathcal{E}_B = \sin\vartheta/r^2$ whose contribution to the energy is the same as $E_{\mathrm{U}(1)}$ with $\nu^2 = 1$ in (4.15).

The total energy is $E = E_{\mathrm{U}(1)} + E_{\mathrm{SU}(2)}$ where

$$E_{\mathrm{SU}(2)} = 4\pi \int_0^\infty \left(\frac{1}{g^2} \left(\frac{\nu^2+1}{2} f'^2 + \nu^2 \frac{(f^2-1)^2}{2r^2} \right) + (r\phi')^2 + \frac{\nu^2+1}{4}(f\phi)^2 + \frac{r^2\beta}{8}(\phi^2-1)^2 \right) dr. \tag{4.16}$$

Unless otherwise stated (the only exception will be made in Section V.E), it will always be assumed in this formula that $\nu^2 = 1$, since only in this case the spherical symmetry can be maintained on-shell. Equations (4.2) then can be obtained by varying $E_{\mathrm{SU}(2)}$ with respect to f, ϕ.

For the Dirac monopole with $\nu^2 = 1$ one has $f = 0$ hence $E_{\mathrm{SU}(2)} = \infty$, but for the CM monopole one obtains a finite value $E_{\mathrm{CM}} \equiv E_{\mathrm{SU}(2)} = 15.759$, assuming that $g'^2 = 1 - g^2 = 0.23$. Therefore, even though the total energy is infinite due to the U(1) field, this solution is less energetic than the Dirac monopole. It is convenient to use the compact coordinate x defined

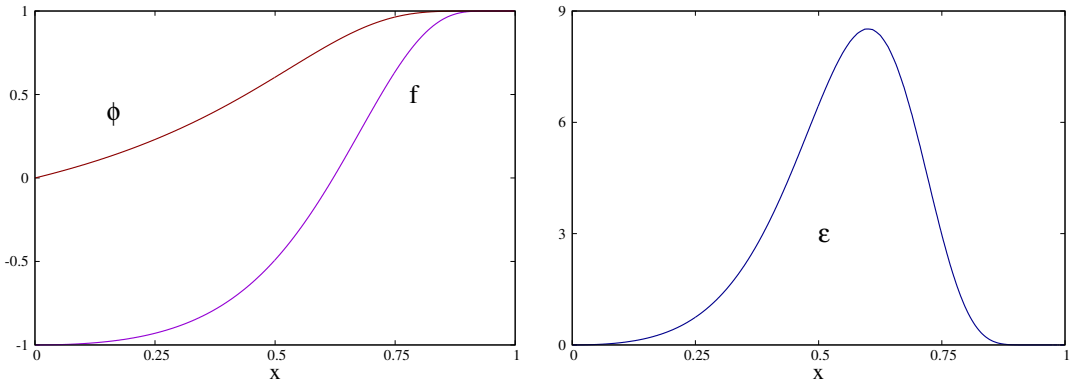


FIG. 2. Profiles of f and ϕ (left) and the energy density (right) against the compact radial coordinate x for the the spherically symmetric sphaleron with $g' = 0$.

in (3.22) to represent the energy as

$$E_{\rm SU(2)} = 4\pi \int_0^1 \varepsilon(x)\, dx\,, \tag{4.17}$$

where the energy density ε is the integrand in (4.16) multiplied by dr/dx. Due to the longe-range magnetic field of the monopole, the integrand in (4.16) decays at large r as $1/r^2$, while $dr/dx \sim r^2$, hence $\varepsilon(x)$ approaches at infinity a constant value $\varepsilon_\infty = 1/(2g^2)$, as seen in Fig.1. As a result, the non-Abelian part of the energy is smoothly distributed in space.

The magnetic charge density is defined in (2.16). Its U(1) part is given by the general formula (3.17) which applies to all monopoles, while the SU(2) part is

$$\rho_{\rm SU(2)} = \frac{1}{4\pi}\,\frac{g'}{g\,r^2}\,(f^2)'\,. \tag{4.18}$$

This determines the SU(2) part of the magnetic charge,

$$P_{\rm SU(2)} = \int \rho_{\rm SU(2)}\sqrt{-{\rm g}}\, d^3x = \nu\,\frac{g'}{g}\int_0^\infty (f^2)' dr = -\nu\,\frac{g'}{g} = -g'^2\,\frac{\nu}{e} = g'^2 P. \tag{4.19}$$

This is the same as $P_{\rm SU(2)}$ with $\nu^2 = 1$ in (4.12), and the U(1) part of the charge is the same $P_{\rm U(1)}$ in (4.12). Therefore, the SU(2) part of the magnetic charge is distributed all over the space while its U(1) part is concentrated at the origin as for the Dirac monopole.

B. Sphaleron

The spherically symmetric CM monopole exists for any value of the weak mixing angle, but the sphaleron can be spherically symmetric only if $g' = 0$ when the U(1) hypercharge field decouples [29, 32]. The solution is obtained by setting in (3.8)

$$\Theta(\vartheta) = 1, \quad H_2 = f(r) - 1, \quad H_3 = H_2\,\sin\vartheta, \quad H_4 = H_2\,\cos\vartheta, \quad \phi_2 = \phi(r), \tag{4.20}$$

with $H_1 = y = \phi_1 = 0$. Notice that this implies that the U(1) field is not zero but a pure gauge, $B = \nu\, d\varphi$. Since the U(1) gauge transformations are still allowed when $g' = 0$, the pure gauge B can be gauged away, but at the expense of giving the Higgs field a φ-depending phase. Therefore, it is preferable to work in the gauge (4.20) where nothing depends on φ.

Injecting (4.20) to the equations, the angular variables decouple yielding

$$\begin{aligned} f'' &= \frac{f(f^2-1)}{r^2} + \frac{1}{2}\,\phi^2(f-1)\,, \\ (r^2\phi')' &= \frac{1}{4}\,(\nu^2+1)(f-1)^2\phi + \frac{\beta r^2}{4}\,(\phi^2-1)\phi\,, \\ (\nu^2-1)f' &= (\nu^2-1)(f-1)\phi = 0. \end{aligned} \tag{4.21}$$

Only trivial solutions are possible for arbitrary ν, but for $\nu^2 = 1$ there is a non-trivial solution with asymptotics $f = -1+\mathcal{O}(r^2)$, $\phi = \mathcal{O}(r)$ as $r \to 0$ and $f = 1+\mathcal{O}\left(e^{-m_{\rm W} r}\right)$, $\phi = 1+\mathcal{O}\left(e^{-m_{\rm H} r}\right)$ for $r \to \infty$ [29, 32]. This solution is show in Fig.2. Its total energy,

$$E = 4\pi \int_0^\infty dr \left(f'^2 + \frac{(f^2-1)^2}{2r^2} + (r\phi')^2 + \frac{1}{2}(f-1)^2\phi^2 + \frac{r^2\beta}{8}(\phi^2-1)^2 \right) \equiv 4\pi \int_0^1 \varepsilon\, dx, \tag{4.22}$$

is finite and evaluates to $E = 33.538$. Since $g' = 0$, the electromagnetic field is zero and the sphaleron does not support long-range fields, hence its energy density $\varepsilon(x)$ approaches zero at infinity, as seen in Fig.2.

V. AXIALLY SYMMETRIC MONOPOLES

The spherically symmetric monopoles of Cho-Maison exists for any $\theta_{\rm W}$ but only for the magnetic charge $P = \pm 1/e$. In order to construct their generalizations for higher values of $|P|$, one should relax the assumption of spherical symmetry. The simplest possibility is to consider axially symmetric fields discussed in Section III. Summarizing the discussion there, here are the boundary conditions for the axially symmetric monopoles:

$$\begin{aligned} \text{axis}\quad \underline{\vartheta = 0}: &\qquad H_1 = H_3 = y = \phi_1 = 0, \qquad \partial_\vartheta H_2 = \partial_\vartheta H_4 = \partial_\vartheta \phi_2 = 0; \\ \text{equator}\quad \underline{\vartheta = \pi/2}: &\qquad H_1 = H_3 = y = \phi_1 = 0, \qquad \partial_\vartheta H_2 = \partial_\vartheta H_4 = \partial_\vartheta \phi_2 = 0; \\ \text{origin}\quad \underline{r = 0}: &\qquad H_1 = H_3 = y = \phi_1 = \phi_2 = 0, \qquad H_2 = H_4 = 1; \\ \text{infinity}\quad \underline{r = \infty}: &\qquad H_1 = H_2 = H_3 = H_4 = y = \phi_1 = 0, \qquad \phi_2 = 1. \end{aligned} \tag{5.1}$$

The conditions at the symmetry axis and in the equatorial plane are determined by (3.9),(3.10), while those at the origin and at infinity are the same as for spherically symmetric monopoles in (4.1). It turns out that when these boundary conditions are fulfilled, the relation $H_2 = H_4$ at the axis mentioned in (3.10) is also fulfilled; we checked this numerically.

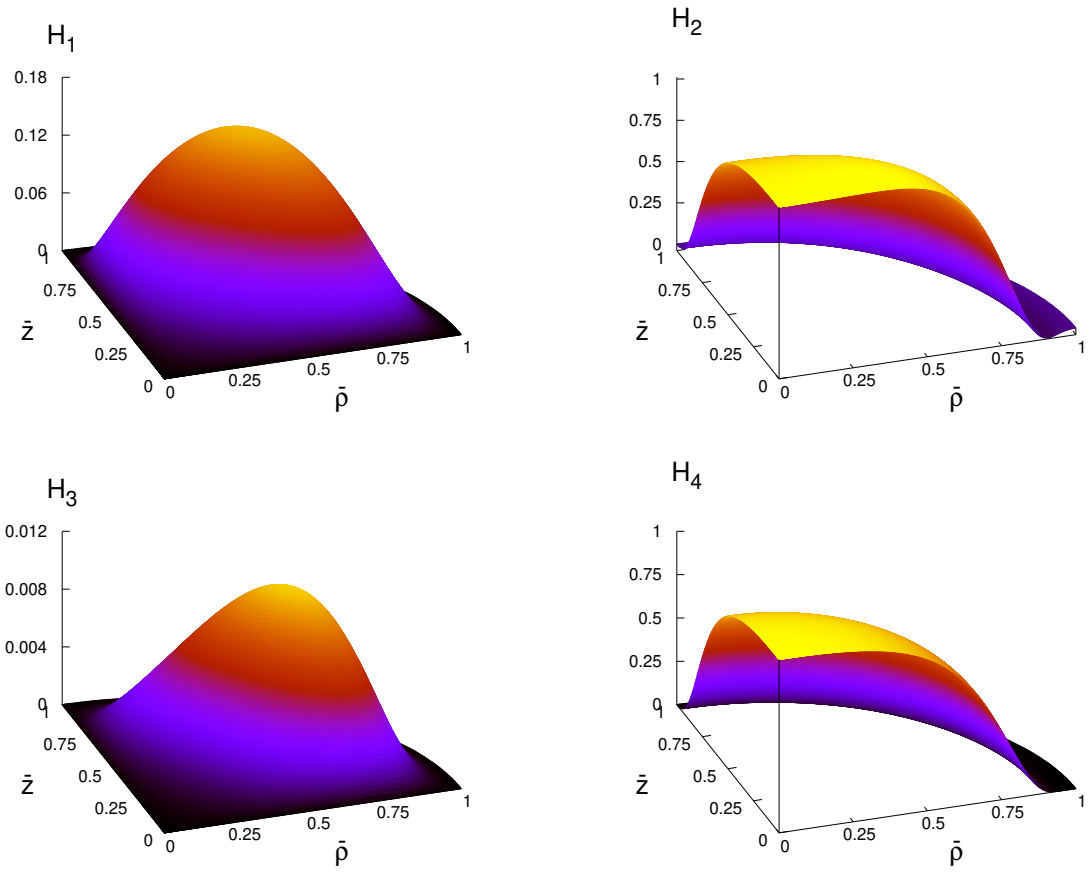


FIG. 3. The SU(2) amplitudes for the $\nu = 2$ monopole solution against $\bar{\rho} = x \sin\vartheta$ and $\bar{z} = x \cos\vartheta$.

Our aim is to solve the field equations with these boundary conditions to determine the components of the "state vector"

$$\Psi = [H_1, H_2, H_3, H_4, y, \phi_1, \phi_2], \tag{5.2}$$

which are functions of r, ϑ. We solve the equations with the FreeFem++ numerical solver based on the finite element method [34]. This solver uses the weak form of differential equations obtained by transforming them into integral equations, expanding with respect to basis functions obtained by triangulating the integration domain, and handling the non-linearities with the Newton-Raphson procedure. The numerical procedure is stable and shows a fast convergence rate on 4 laptop parallel processors.

The equations contain the parameter ν, and for $\nu = 1$ the solution is known – this is the spherically symmetric CM monopole for which

$$\underline{\nu = 1}: \qquad H_1 = H_3 = y = \phi_1 = 0, \qquad H_2 = H_4 = f(r), \qquad \phi_2 = \phi(r), \tag{5.3}$$

with $f(r)$ and $\phi(r)$ shown in Fig.1. We use this solution as the starting point in the iterative procedure to change the value of ν. Of course, ν should be integer for the line singularities

in the fields to be absent, but the equations can be solved any real ν. Our numerical scheme converges well for $\nu \neq 1$ and we were able to go as far as $\nu = 100$, after which the virial relation deteriorates. The latter is defined as follows.

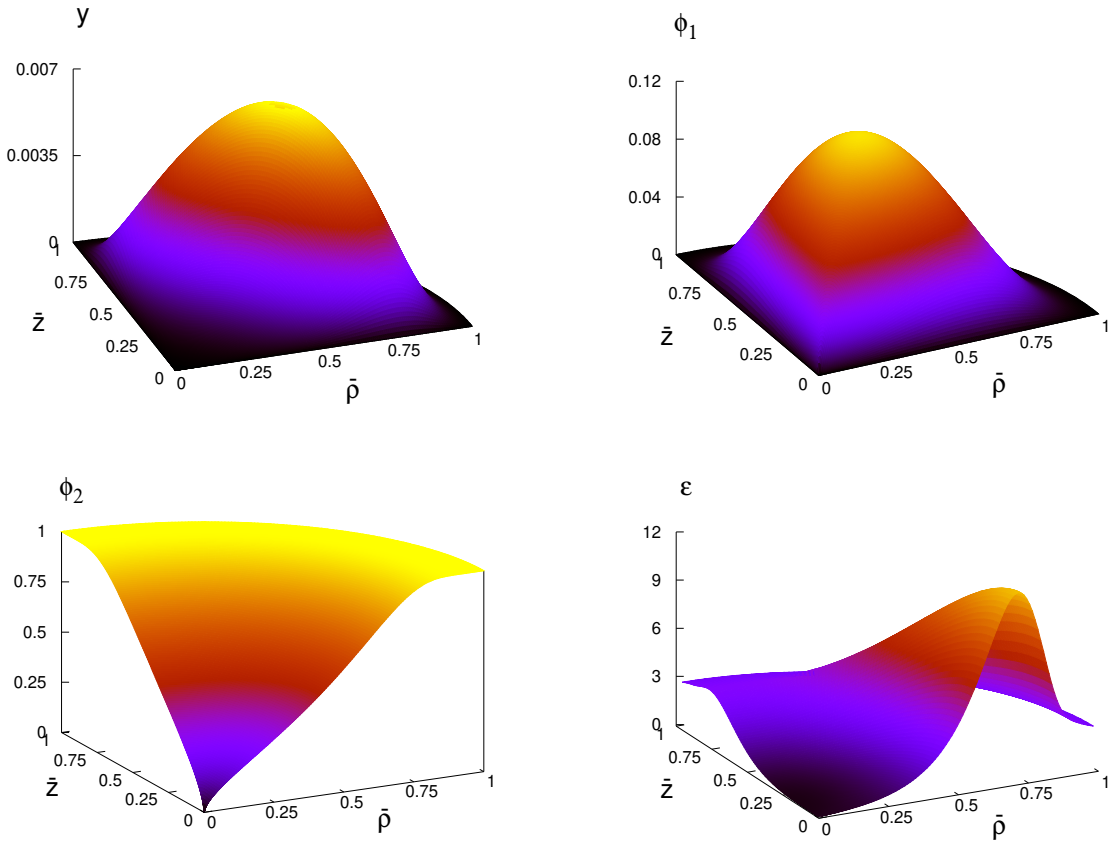


FIG. 4. The U(1) and Higgs amplitudes and the energy density for the $\nu = 2$ monopole solution.

A. Virial relation

The energy (3.4) is infinite due to the contribution of the U(1) term $\mathcal{E}_B$. Since $Y = \cos\vartheta + y\sin\vartheta$, one has

$$\mathcal{E}_B = \left((\partial_r Y)^2 + \frac{1}{r^2}(\partial_\vartheta Y)^2\right)\frac{\nu^2}{\sin\vartheta} = \frac{\nu^2}{r^2}\sin\vartheta + \dots , \tag{5.4}$$

and injecting this to (3.4) yields

$$E = \int T_{00}\sqrt{-g}\, d^3x = \frac{2\pi\nu^2}{g'^2}\int_0^\infty \frac{dr}{r^2} + E_{\rm reg} \equiv E_{\rm U(1)} + E_{\rm reg}. \tag{5.5}$$

Here the first term on the right is infinite and is the same as $E_{\rm U(1)}$ in the energy (4.15) of the pointlike monopole. The second term on the right, $E_{\rm reg}$, is finite and contains the finite part of the U(1) contribution, denoted by the dots in (5.4), and also contributions of the SU(2)

and Higgs fields. In other words, $E_{\rm reg}$ is the regularized energy obtained by subtracting the divergent term $E_{\rm U(1)}$. It is determined by the state vector Ψ,

$$E_{\rm reg}[\Psi] \equiv 2\pi \int_0^\pi \sin\vartheta \, d\vartheta \int_0^1 \varepsilon(x,\vartheta)\, dx\,, \tag{5.6}$$

which reduces to (4.16) with $\nu^2 = 1$ for the spherically symmetric field (5.3). The field equations determining the state vector Ψ are obtained by varying the total energy $E = E_{\rm U(1)} + E_{\rm reg}$, but they can equally be obtained by varying only $E_{\rm reg}$,

$$\frac{\delta E_{\rm reg}[\Psi]}{\delta \Psi} = 0, \tag{5.7}$$

since $E_{\rm U(1)}$ does not depend on Ψ. If $\Psi(r,\vartheta)$ is a solution then $E_{\rm reg}$ should be stationary with respect to the rescaling $r \to \lambda\, r$, which leads to the virial relation,

$$v \equiv \frac{d}{d\lambda} \ln E_{\rm reg}[\Psi(\lambda\, r,\vartheta)]\Big|_{\lambda=1} = 0. \tag{5.8}$$

This relation is fulfilled for all our solutions with a precision depending on the numbers of the discretization points N_x and N_ϑ along the x, ϑ axes (these numbers determine the triangulation pattern for the FreeFem++ solver). Taking $N_x = 100$ and $N_\vartheta = 50$ yields typically $v \sim 10^{-8}$ or $v \sim 10^{-7}$.

B. Solutions

The profiles of the $\nu = 2$ solution are shown in Fig.3 and Fig.4. The functions H_2, H_4, ϕ_2 which do not vanish in the spherically symmetric limit $|\nu| = 1$ remain essentially the same for $|\nu| > 1$ and almost do not depend on the angle ϑ. The most notable change is that ϕ_2 now faster approaches zero at the origin, as described by Eq.(5.9) below, whereas H_2 is not strictly positive. On the other hand, the functions H_1, H_3, y, ϕ_1 which vanish for $\nu^2 = 1$ no longer vanish for $\nu^2 > 1$ and show a strong ϑ-dependence. The norm of Higgs field $|\Phi|$ vanishes at the origin.

The energy density ε defined in (5.6) depends only on the radial coordinate for $\nu = \pm 1$, but already for $\nu = 2$ it shows a strong ϑ-dependence with a marked maximum in the vicinity of the equatorial plane, as seen in Fig.4 and in Fig.5. It is interesting that ε is actually not positive definite and can assume negative values in the central region, although the total energy density T_{00} including the unbounded $U(1)$ contribution is of course always positive.

The profiles of the energy density $\varepsilon(x,\vartheta)$ for fixed values of ϑ in Fig.5 show that ε is an almost monotone function of the radial coordinate along the symmetry axis at $\vartheta = 0$, but it shows a marked maximum along the equatorial plane for $\vartheta = \pi/2$. This implies that surfaces

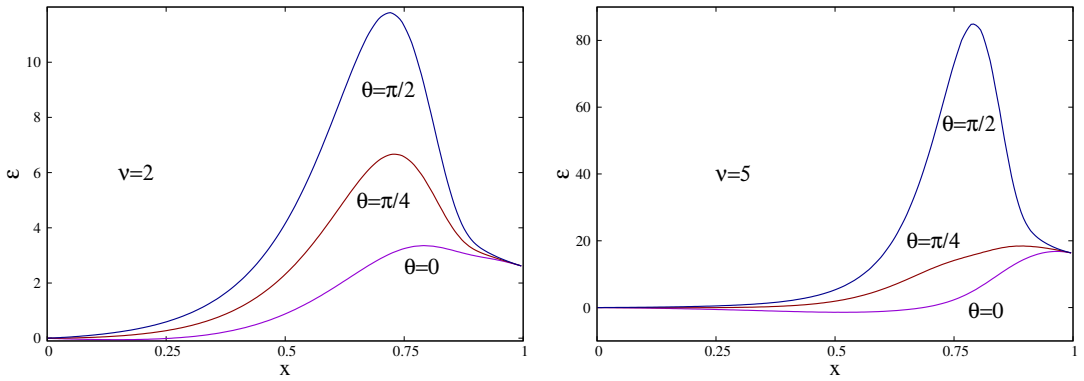


FIG. 5. The energy density $\varepsilon(x, \vartheta)$ for several fixed values of ϑ for $\nu = 2$ (left) and for $\nu = 5$ (right). In the latter case the maximum is much higher.

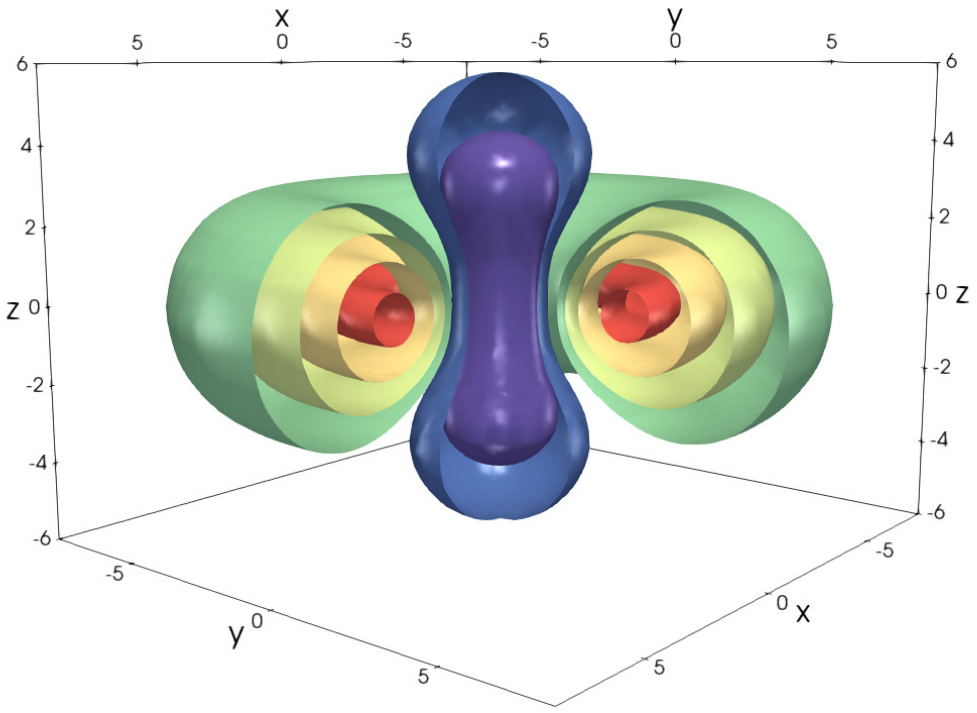


FIG. 6. Surfaces of constant energy density $\varepsilon = \varepsilon_0$ for the $\nu = 5$ monopole solution expressed in Cartesian coordinates x, y, z. For small values of ε_0 the surfaces are deformed ellipsoids but for larger ε_0 they become tori.

of constant energy density $\varepsilon(x, \vartheta) = \varepsilon_0$ are similar to ellipsoids if ε_0 is small, but for larger values of ε_0 they assume toroidal form, which indeed can be seen in Fig.6.

Solutions with $\nu > 2$ have essentially the same structure as the $\nu = 2$ solution. The functions H_2, H_4, ϕ_2 always depend only weakly on the polar angle ϑ while H_1, H_3, y, ϕ_1 show more and more pronounced extrema when ν increases. The Higgs field vanishes only at the

ν	1/2	1	2	3	4	5
$E_{\rm reg}$	6.94	15.76	38.12	65.76	97.92	134.13
q	− 0.51	0	3.66	10.61	20.68	33.78

TABLE I. The energy $E_{\rm reg}$ and quadrupole moment q for several monopole solutions.

origin, and close to the origin one has

$$\phi_1 \sim \phi_2 \sim r^\lambda \quad \text{with} \quad \lambda = \frac{\sqrt{1+2\nu}-1}{2}\,, \tag{5.9}$$

as explained in Appendix B. The energy density gets more and more concentrated in the equatorial region and attains higher and higher values there. This can be seen in Fig.5 where the density ε is shown for $\nu = 2$ and $\nu = 5$. The numerical values of the regularized energy $E_{\rm reg}$ for several values of the winding number ν are shown in Table I. We include for completeness also the $\nu = 1/2$ solution because it corresponds to the minimal value of the magnetic charge $|n| = 2|\nu| = 1$, but one should remember that this solution contains the line singularity.

Many technical details, as for example the asymptotic structure of the solutions at infinity, solutions at the origin, are given in the two Appendices.

C. The interior structure

The profiles functions $H_1, H_2, H_3, H_4, y, \phi_1, \phi_2$ of the solutions and the energy density are insensitive to the sign of ν, so that for example, they are the same for $\nu = 2$ and $\nu = -2$. On the other hand, the electromagnetic field in (2.13) and hence the electric and magnetic currents in (2.15) do depend on the sign of ν.

Fig.7 shows the magnetic charge density and the electric current density for the $\nu = 2$ monopole. The magnetic charge splits as $P = P_{\rm U(1)} + P_{\rm SU(2)}$ according to (2.17), where the U(1) part is pointlike and given by (3.17), while the SU(2) part is

$$P_{\rm SU(2)} = \int \rho_{\rm SU(2)} \sqrt{-\rm g}\, d^3x \equiv 2\pi \int_0^\pi \sin\vartheta\, d\vartheta \int_0^1 Q(x,\vartheta)\, dx\,. \tag{5.10}$$

This part of the charge is smoothly distributed over the space, but its value is the same as for the pointlike monopole, $P_{\rm SU(2)} = -g'^2\nu/e = -\nu g'/g$, and the numerical verification of this is a good consistency check for our procedure. What is interesting is the profile of the charge distribution $Q(x,\vartheta)$. For $\nu = \pm 1$ when the monopole is spherically symmetric, comparing with (4.19) yields

$$\nu = \pm 1: \qquad Q = \frac{\nu g'}{4\pi g}\left(f^2\right)'_x\,, \tag{5.11}$$

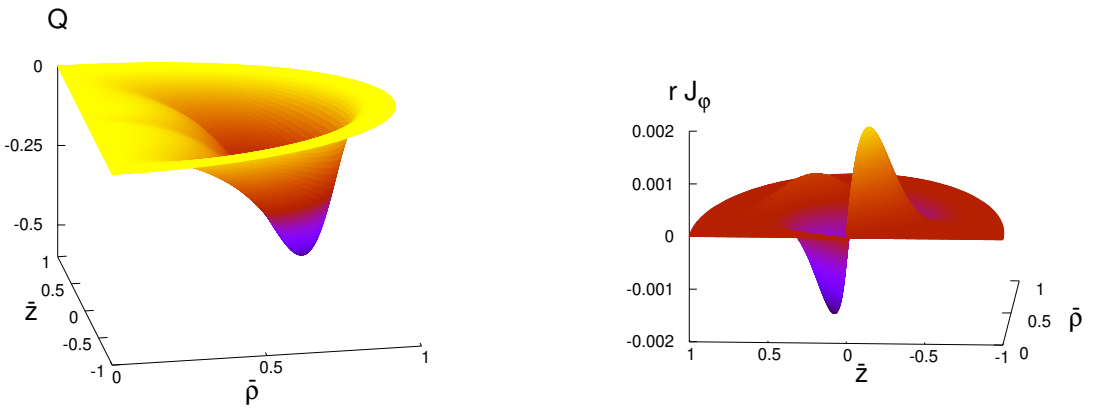


FIG. 7. The magnetic charge and electric current densities for the $\nu = 2$ monopole solution.

hence Q depends only on the radial coordinate. Therefore, the SU(2) part of the charge density for the CM monopole is uniformly distributed over the 2-sphere. However, already for $\nu = 2$ the charge density is not at all spherical and shows a strong ϑ-dependence with a profound minimum at the equatorial plane some distance away from the origin, as seen in Fig.7. This implies that the magnetic charge distribution has a toroidal shape with the maximal value along a ring in the equatorial plane at $z = 0$. Solutions with higher ν show a similar toroidal structure of the charge density.

The electric current density J^μ vanishes for the CM monopole, but for $|\nu| > 1$ it has a non-zero azimuthal component J_φ. The total current through the $\rho - z$ half-plane is zero, $I = I_+ + I_- = 0$, but the currents in the $z > 0$ and $z < 0$ regions,

$$I_+ = \int_0^\infty dz \int_0^\infty (\vec{J} \cdot \vec{n}_\varphi)\, \rho \, d\rho \,, \qquad I_- = \int_{-\infty}^0 dz \int_0^\infty (\vec{J} \cdot \vec{n}_\varphi)\, \rho \, d\rho \,, \tag{5.12}$$

do not vanish. Here $\vec{n}_\varphi$ is the unit vector in the azimuthal direction. Therefore, the monopole contains inside two oppositely directed circular electric currents, which can be viewed as a manifestation of the electroweak superconductivity [41, 42]. One has $J_\varphi \sim 1/r$ close to the origin, which does not affect the convergence of the integrals in (5.12) but complicates the graphical representation of J_φ. Therefore, we show in the plots the bounded product rJ_φ. As seen in Fig.7, J_φ is antisymmetric with respect to the reflection in the equatorial plane, with a profound minimum in the upper hemisphere and a marked maximum in the lower hemisphere. This corresponds to two superconducting azimuthal currents flowing in opposite directions and giving rise to two oppositely oriented magnetic moments.

Fig.8 shows level surfaces for the SU(2) charge density Q defined in (5.10) and for the current density rJ_φ for the $\nu = 2$ and $\nu = 4$ monopole solutions. The thick toroidal region containing the equatorial plane (green online) contains the non-Abelian magnetic charge. Al-

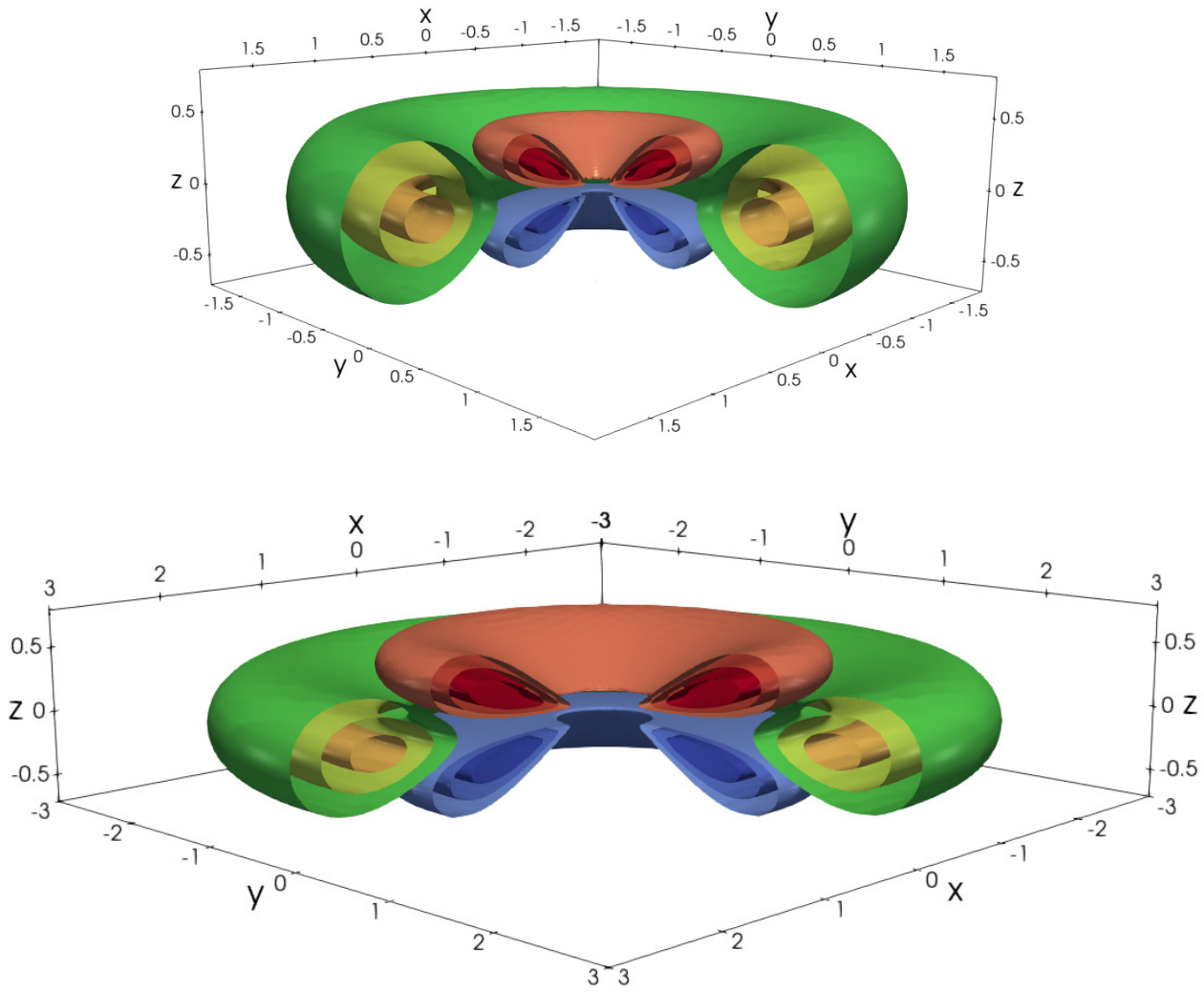


FIG. 8. Surfaces of constant magnetic charge and electric current densities for the $\nu = 2$ (upper panel) and $\nu = 4$ (lower panel) monopole solutions in Cartesian coordinates of the 3-space. The ring radii in the latter case are twice as large, but their thickness is the same.

though solutions with $\nu > 1$ can be thought of as superpositions of ν Cho-Maison monopoles, these monopoles cannot be distinguished from each other and merge together into a toroidal condensate. At the same time, the Higgs field vanishes only at the origin. The other two tori shown in Fig.8 above and below the equatorial plane (red and blue online) correspond to two oppositely directed distributions of the azimuthal electric current – superconducting rings. As is seen in Fig.8, the whole picture is qualitatively the same for $\nu = 2$ and for $\nu = 4$, and the same picture is found for other (even or odd) values of ν.

All of this suggests the following qualitative description of the inner structure of the multi-monopole solutions. The SU(2) part of their magnetic charge is distributed over the volume of a magnetically charged ring (the U(1) part of the charge is always located at the origin).

The magnetic ring creates a magnetic field which is mostly anti-parallel to the z-axis for $z > 0$ (assuming that $\nu > 0$, the charge of the ring then being negative) and mostly parallel to the axis in the $z < 0$ region. This magnetic field forces the electrically charged W-bosons constituting the condensate inside the monopole to Larmore orbit in one direction for $z > 0$ and in the opposite direction for $z < 0$. This produces two circular superconducting electric currents. These currents produce two oppositely oriented magnetic dipole moments repelling each other but attracted to the magnetic ring. Each dipole creates a magnetic field directed oppositely to that of the magnetic ring (Lenz's law), hence pushing the individual CM monopoles (or rather their SU(2) charges) contained in the ring toward the equatorial plane. This field overcomes the mutual repulsion of the individual monopoles and squeezes them into a toroidal condensate.

Of course, this electromagnetic analogy cannot be totally adequate since the electromagnetic description applies only in the Higgs vacuum, whereas the Higgs field is not in vacuum inside the monopole. However, the analogy is suggestive.

D. Quadrupole moment

The electromagnetic analogy shows that the total magnetic dipole moment of the monopole is zero. Indeed, its dipole moments generated by the currents $I_\pm$ have opposite signs and compensate each other, while the magnetic charge density is everywhere sign definite. However, the magnetic quadrupole moment does not vanish. The latter is described by the traceless tensor q_{ik} receiving contribution from the magnetic charge and electric current [43],

$$q_{ik} = \int \left[3x_i x_k - r^2\delta_{ik}\right]\, \rho_{\mathrm{SU(2)}}\, d^3x + \int \left[x_i\,(\vec{r}\wedge\vec{J})_k + x_k\,(\vec{r}\wedge\vec{J})_i\right] d^3x\,, \tag{5.13}$$

where $x_k = (x, y, z)$ are Cartesian coordinates. Owing to the axial symmetry, the tensor has the structure $q_{ik} = \mathrm{diag}[-q/2, -q/2, q]$, where the only independent component,

$$q = q_{zz} = \int \left[3z^2 - r^2\right]\, \rho_{\mathrm{SU(2)}}\, d^3x + \int 2zJ_\varphi\, d^3x, \tag{5.14}$$

determines the deviation from the spherical symmetry. The first integral here gives the dominant contribution and for the *oblate* systems shown in Fig.8 one has $q > 0$ since $\rho_{\mathrm{SU(2)}}$ is negative when ν is positive. We can get the value of q from our solutions as follows. The quadrupole moment (5.13) determines the asymptotic form of the non-spherically symmetric part of the magnetic field [43],

$$\delta\mathcal{B}_i = \frac{1}{2r^7}\left[5\,x_i x_j x_k - r^2\,(x_i\delta_{jk} + x_j\delta_{ik} + x_k\delta_{ij})\right] q_{jk}\,, \tag{5.15}$$

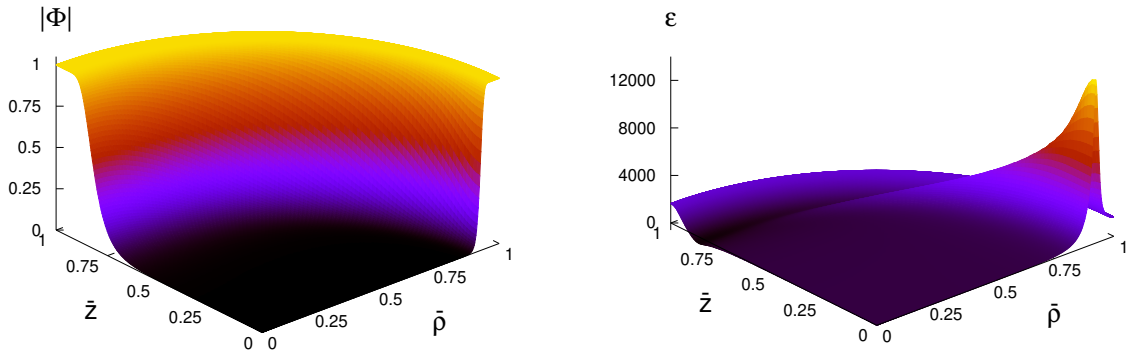


FIG. 9. The norm of the Higgs field $|\Phi|$ and the energy density ε for the monopole solution with $\nu = 50$.

(the spherically symmetric part of the magnetic fields is the Dirac monopole (4.8)). In the axially symmetric case, passing to spherical coordinates, this reduces to

$$\delta\mathcal{B} = \frac{3q}{4r^4}\left[(3\cos^2\vartheta - 1)\,dr + r\sin(2\vartheta)\,d\vartheta\right]. \tag{5.16}$$

On the other hand, as shown by (A.11) in Appendix A, the asymptotic form of the electromagnetic vector potential is

$$\delta\mathcal{A} = \frac{\nu}{gg'}\,y_\gamma\,\sin\vartheta\,d\varphi = \frac{\nu}{gg'}\,\frac{C_\gamma}{r^2}\sin^2\vartheta\cos\vartheta\,d\varphi\,, \tag{5.17}$$

where the value of the coefficient C_γ is determined by the numerics. Computing then the magnetic field $\delta\vec{\mathcal{B}} = \vec{\nabla}\wedge\delta\vec{\mathcal{A}}$ yields exactly the same expression as in (5.16), with

$$q = \frac{4\,\nu}{3\,gg'}\,C_\gamma\,. \tag{5.18}$$

We can therefore read-off the quadrupole moment from the asymptotic form of our solutions, and its values for the lowest ν are shown in Table I. One can see that q increases with ν, which corresponds to the fact that the oblateness of the solutions increases with growing magnetic charge. On the other hand, q becomes negative for $\nu < 1$, and we checked that solutions become *prolate* in this case, with magnetic density levels surfaces stretched along the z-axis.

E. The limit of large magnetic charge

Increasing the winding number ν, we could obtain solutions up to $\nu = 100$ while keeping small the virial v in (5.8). Both the energy $E_{\rm reg}$ and quadrupole moment q always increase with ν. One can use the following arguments to obtain analytical estimates.

It is known that when the magnetic field becomes very strong, then the Higgs field approaches zero and the full electroweak gauge symmetry is restored [44, 45]. This can be seen in the inner structure of the classical solutions [41, 42]. In our case, when the magnetic charge P increases the magnetic field gets stronger, hence the Higgs field in the central region of the monopole is expected to approach zero. This expectation is confirmed already by the perturbative analysis since close to the origin one has (see Appendix B)

$$\phi_1 \sim r^\lambda \left[\left(\sin \frac{\vartheta}{2} \right)^{\nu+1} + \left(\cos \frac{\vartheta}{2} \right)^{\nu+1} \right] , \quad \phi_2 \sim \partial_\vartheta \phi_1 \, , \tag{5.19}$$

with $\lambda = (\sqrt{1+2\nu} - 1)/2$, hence the Higgs gets smaller when ν increases.

The numerical analysis confirms the expectation at the non-perturbative level and shows that for large ν the monopoles develop in the central region a spheroidal bubble where the norm of the Higgs field $|\Phi| = \sqrt{\phi_1^2 + \phi_2^2}$ is very close to zero, hence the system is in the false vacuum. This can be seen in Fig.9 for $\nu = 50$. The SU(2) gauge field also vanishes in the bubble, since H_1, H_3 are very close to zero while H_2, H_4 are very close to unity, in which case one has $W_\mu^a = 0$, as seen in (3.12). The y amplitude is very close to zero too. As a result, inside the bubble there remains only the U(1) hypercharge field,

$$\underline{\text{inside:}} \quad B_\mu dx^\mu = \nu \, (\cos\vartheta \pm 1) d\varphi \, , \qquad W_\mu^a = 0, \qquad \Phi = 0. \tag{5.20}$$

In view of (2.13), this describes the electromagnetic field $F_{\mu\nu} = (g/g') \, B_{\mu\nu}$ of the pointlike magnetic charge $P_{\mathrm{U}(1)} = -\nu g/g'$ and the Z-field $Z_{\mu\nu} = B_{\mu\nu}$. Since the gauge symmetry is restored, the Z-field is massless.

Outside the bubble, the Higgs field approaches the vacuum value $|\Phi| = 1$ generating non-zero masses for the fields, and being massive, the latter tend to zero at large distances exponentially fast. The monopole configuration then approaches that in (4.5),

$$\underline{\text{outside:}} \quad B_\mu dx^\mu = \nu \, (\cos\vartheta \pm 1) \, d\varphi, \qquad \mathrm{T}_a W_\mu^a = \mathrm{T}_3 \, B_\mu dx^\mu, \qquad \Phi = \begin{pmatrix} 0 \\ 1 \end{pmatrix} . \tag{5.21}$$

This corresponds to the Dirac monopole of charge $P_{\mathrm{U}(1)} + P_{\mathrm{SU}(2)} = -\nu/e$.

The Higgs field interpolates between $|\Phi| = 0$ and $|\Phi| = 1$ in the "bubble crust" – a transition region between the inside and outside. This region contains a W-condensate in the form of rings close to the equatorial plane, as shown in Fig.10 for $\nu = -20$. The condensate generates a magnetic charge and electric currents. Comparing with the similar picture in Fig.8, one can see that the rings become large and strongly squashed for large $|\nu|$, while their thickness in the z direction visibly does not change. The total non-Abelian magnetic charge contained in the crust is $P_{\mathrm{SU}(2)} = -\nu g'/g$.

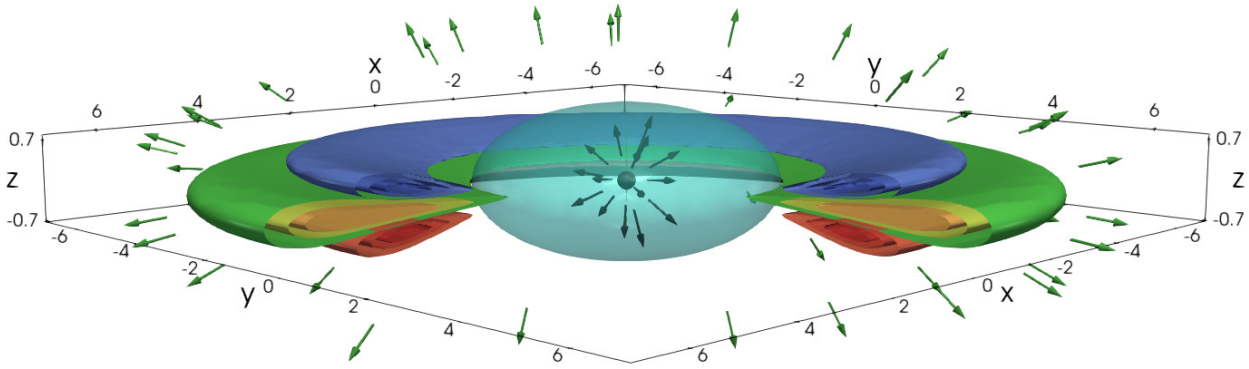


FIG. 10. Profiles of the magnetic monopole solution for $\nu = -20$. The central region is occupied by a spheroidal bubble (cyan online) containing the U(1) hypercharge field generated by a pointlike magnetic charge $P_{\mathrm{U}(1)} = -\nu g/g'$ in the center. This field is strong enough to suppress all other fields. Outside the bubble, the non-linear fields emerge from vacuum and produce a condensate forming a ring of non-Abelian magnetic charge $P_{\mathrm{SU}(2)} = -\nu g'/g$ squeezed between two superconducting rings of opposite electric currents. Still farther away, the non-linear fields die away and there remains only the magnetic field of the Dirac monopole of total charge $P_{\mathrm{U}(1)} + P_{\mathrm{SU}(2)} = -\nu/e$.

Although the bubble is not exactly spherical (this is seen already in Fig.9), reasonable estimates can be obtained via approximating the fields by the spherically symmetric expressions (4.1) with the profile functions $f(r), \phi(r)$,

$$f(r) = 1 \quad \text{if} \quad r < R, \qquad f(r) = 0 \quad \text{if} \quad r > R, \qquad \phi(r) = 1 - f(r). \tag{5.22}$$

Injecting this to Eq.(4.16) where ν is kept arbitrary, yields the energy

$$E_{\mathrm{reg}} = E_{\mathrm{SU}(2)} = \frac{\beta}{8}\,\frac{4\pi R^3}{3} + 4\pi\,\frac{\nu^2}{2g^2 R}\,. \tag{5.23}$$

Here the first term is the contribution of the constant Higgs energy density inside the bubble, and the second one is the non-Abelian magnetic energy outside the bubble. Minimizing with respect to R, yields the following estimates for the bubble size and energy,

$$R = \left(\frac{4}{\beta g^2}\right)^{1/4}\sqrt{\nu} = 1.29\,\sqrt{|\nu|}\,, \qquad E_{\mathrm{reg}} = \frac{8\pi}{3}\left(\frac{\beta}{4g^2}\right)^{1/4}\nu^{3/2} = 7.4\,|\nu|^{3/2}. \tag{5.24}$$

We can identify the bubble size and hence the position of the bubble crust with the position of the minimum of the function Q shown in Fig.7. The numerically obtained values of the bubble size are in a good agreement with R in (5.24). Moreover, as seen in Fig.11, the numerically obtained ratio $E_{\mathrm{reg}}/\nu^{3/2}$ indeed approaches for large ν a constant value. This value, 11.4, is larger than 7.4 suggested by formula (5.24), but this is because the above analytical estimates

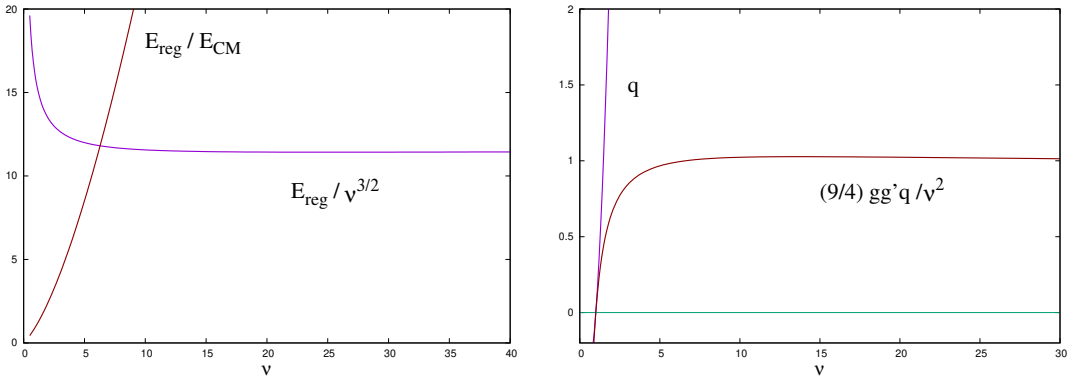


FIG. 11. Left: energy $E_{\rm reg}(\nu)$ in units of the CM monopole energy $E_{\rm CM} = E_{\rm reg}(1)$ and $E_{\rm reg}(\nu)$ divided by $\nu^{3/2}$. Right: the quadrupole moment q and also q divided by $4\nu^2/(9gg')$ against the winding number ν.

take into account only the energy inside and outside the bubble without considering the energy in the crust. More accurate estimates can be obtained by introducing a finite transition region where $f(r)$ and $\phi(r)$ interpolate between the inside and outside values.

Our numerics suggest that for large ν the constant in the asymptotic formula (A.11) approaches the value $C_\gamma = \nu/3$, hence the quadrupole moment defined by (5.18) is

$$q = \frac{4}{9\,gg'}\,\nu^2\,, \tag{5.25}$$

which is clearly seen in Fig.11. This can be represented as

$$q = -\frac{4\,\nu}{9g'^2}\,P_{\rm SU(2)} = -1.16\times P_{\rm SU(2)}R^2\,, \tag{5.26}$$

with R given by (5.24). Therefore

$$q \approx -P_{\rm SU(2)}R^2\,, \tag{5.27}$$

which is the quadrupole moment of a homogeneously charged torus of radius R and charge $P_{\rm SU(2)}$. This shows again that the above estimate for the bubble size R is sensible, because the quadrupole moment in the formula (5.14) is dominated by the magnetic charge density, while the relative contribution of the electric current is negligible for large $|\nu|$. Specifically, the currents $I_\pm$ defined by (5.12) approach finite values $I_\pm = \mp 0.095$ for large ν. Since the radius R of the superconducting rings is proportional to $\sqrt{\nu}$, the dipole moment produced by each rings scales as $\pi R^2 I_\pm \propto \nu$. The dipole moments produced by I_+ and I_- are separated in space and their fields do not exactly compensate each other but produce a quadrupole moment, but since their separation is almost independent on ν, their quadrupole moment grows slower than ν^2 and is sub-dominant as compared to that produced by the magnetic ring.

Since the hypercharge field (5.20) in the monopole center is spherically symmetric, one can wonder why the rest of the configuration should be squashed ? Remember, however,

that the only spherically symmetric solution for a large winding number ν is the Abelian Dirac monopole. All other solutions with the same far field asymptotic are non-Abelian and non-spherically symmetric. If they are axially symmetric, then, as shown by Eq.(A.12) in Appendix A, the angular dependence of the W-modes in the far field zone is given in terms of the Legendre polynomials $P_j^\nu(\cos\vartheta)$ and $P_j^{\nu\pm1}(\cos\vartheta)$. Since $\nu\pm1\approx\nu$ for large ν and since the leading contribution corresponds to the minimal value of $j=|\nu|$, the angular dependence of the W-modes is given by

$$P^\nu_{|\nu|}(\cos\vartheta)\propto(\sin\vartheta)^{|\nu|}\,. \tag{5.28}$$

These modes are strongly localized around $\vartheta=\pi/2$, which agrees with the rings in the equatorial region shown in Fig.10. On the other hand, the angular dependence of the Z, Higgs, and electromagnetic modes is different. It follows that the electric currents in the two superconducting rings and the SU(2) magnetic charge in the central ring must be supported mainly by a condensate of W-bosons.

It is also worth reminding that the Dirac monopole is unstable with respect to perturbations with angular momentum $j=|\nu|-1$ and the instability resides in the W-sector [26]. The Dirac monopole can be viewed as a superposition of two pointlike charges, $P_{\mathrm{U}(1)}$ and $P_{\mathrm{SU}(2)}$. It seems plausible that the instability growth affects the SU(2) field configuration by radiating away all its central part, and what remains condenses to the rings squashed according to (5.28). The total magnetic charge does not change but its SU(2) part no longer remains in the center and gets distributed over the volume of the ring. Of course, there remains to demonstrate that non-Abelian monopoles for $|\nu|>1$ are indeed stable, in which case they may be viewed as remnants of collapse of the Dirac monopoles, but at least for $|\nu|=1$ the proof is available [26].

Although we cannot claim that monopoles with $|\nu|>1$ are stable, we believe this is indeed the case. The stability of the $\nu=\pm1$ CM monopoles was established via an involved partial wave analysis that applies only in the spherically symmetric case [26], but it seems that a different strategy could be used for multi-monopoles. Indeed, it suffices to show that the regularized energy functional $E_{\mathrm{reg}}[\Psi]$, or more precisely its full 3D version, admits a non-trivial minimum in the sector with a fixed SU(2) charge $P_{\mathrm{SU}(2)}$. This can probably be done via a numerical minimization of the energy functional in a 3D domain. However, such an analysis requires separate studies.

VI. SPHALERONS AND THEIR INTERNAL STRUCTURE

Electroweak sphalerons at finite mixing angle have been much studied. These are the fundamental $\nu = 1$ sphaleron [27, 28], the multi-sphalerons with $|\nu| > 1$ [46, 47], the sphaleron-antisphaleron pairs [37, 48], and also spinning sphalerons [38, 39, 49]. We have reproduced the multi-sphalerons with $\nu = 1, 2, \ldots$, mainly to make sure that our procedure is correct, but also to compare their inner structure with that of monopoles.

To obtain the sphaleron solutions, we use the same parameterization (3.8) of the field amplitudes as for the monopoles, but with $\Theta(\vartheta) = 1$ instead of $\Theta(\vartheta) = \cos\vartheta$. The boundary conditions at $\vartheta = \pi/2$ and at $\vartheta = 0$ are provided, respectively, by (3.9) and (3.10), while those at $r = 0, \infty$ should be the same as for the spherically symmetric sphaleron (4.20):

$$\begin{aligned}
\text{axis}\quad \underline{\vartheta = 0}: &\quad H_1 = H_3 = y = \phi_1 = 0, \qquad \partial_\vartheta H_2 = \partial_\vartheta H_4 = \partial_\vartheta \phi_2 = 0;\\
\text{equator}\quad \underline{\vartheta = \pi/2}: &\quad H_1 = H_4 = \phi_1 = 0, \qquad \partial_\vartheta H_2 = \partial_\vartheta H_3 = \partial_\vartheta y = \partial_\vartheta \phi_2 = 0;\\
\text{origin}\quad \underline{r = 0}: &\quad H_1 = y = \phi_1 = \phi_2 = 0, \qquad H_2 = -2, \quad H_3 = -2\sin\vartheta, \qquad H_4 = -2\cos\vartheta;\\
\text{infinity}\quad \underline{r = \infty}: &\quad H_1 = H_2 = H_3 = H_4 = y = \phi_1 = 0, \qquad \phi_2 = 1.
\end{aligned} \tag{6.1}$$

One can directly work with these boundary conditions, but they are singular at the origin where H_3, H_4 remain ϑ-dependent, whereas $r = 0$ is a single point in space where nothing should depend on ϑ. Alternatively, one can perform the gauge transformation (3.3) with the parameter $\chi = 2\vartheta$. This does not affect the gauge condition (3.20), while the spherically symmetric sphaleron configuration (4.20) transforms to

$$H_2 = f(r) + 1, \quad H_3 = -H_2\,\sin\vartheta, \quad H_4 = H_2\,\cos\vartheta, \quad \phi_1 = \phi(r)\sin\vartheta, \quad \phi_2 = \phi(r)\cos\vartheta, \tag{6.2}$$

and $H_1 = y = 0$. Since $f(0) = -1$ and $\phi(0) = 0$, all field amplitudes now vanish at $r = 0$. The boundary conditions for axially symmetric fields then become

$$\begin{aligned}
\text{axis}\quad \underline{\vartheta = 0}: &\quad H_1 = H_3 = y = \phi_1 = 0, \qquad \partial_\vartheta H_2 = \partial_\vartheta H_4 = \partial_\vartheta \phi_2 = 0;\\
\text{equator}\quad \underline{\vartheta = \pi/2}: &\quad H_1 = H_4 = \phi_2 = 0, \qquad \partial_\vartheta H_2 = \partial_\vartheta H_3 = \partial_\vartheta y = \partial_\vartheta \phi_1 = 0;\\
\text{origin}\quad \underline{r = 0}: &\quad H_1 = H_2 = H_3 = H_4 = y = \phi_1 = \phi_2 = 0;\\
\text{infinity}\quad \underline{r = \infty}: &\quad H_1 = y = 0, \quad H_2 = 2, \quad H_3 = -2\,\sin\vartheta, \quad H_4 = 2\,\cos\vartheta,\\
&\quad \phi_1 = \sin\vartheta, \quad \phi_2 = \cos\vartheta.
\end{aligned} \tag{6.3}$$

This corresponds to the gauge originally used in [27, 28]. The ϑ-dependence is now moved to large values of r where it causes no problems. Notice that ϕ_2 becomes odd under the reflection $\vartheta \to \pi - \vartheta$ while ϕ_1 is even.

Using either (6.1) or (6.3) with, respectively, either (4.20) or (6.2) as the input configuration, our numerical scheme converges giving sphaleron solutions for any ν and $\theta_{\rm W}$. We obtain the same results as those previously reported [27, 28, 47], hence we do not show them and concentrate on the analysis of the inner sphaleron structure. The latter can be studied as for the monopoles via analysing the electric and magnetic charge densities (2.15). In the sphaleron case there is an additional way of doing this since, unlike the monopoles, the fundamental sphaleron with $\nu = 1$ and $\sin^2\theta_{\rm W} = 0.23$ is only slightly non-spherical, in which case the perturbative approach is possible. Specifically, the amplitudes $H_2, H_3, H_4, \phi_1, \phi_2$ are well described by the spherically symmetric formula (6.2) with $f(r), \phi(r)$ shown in Fig.2, and the most notable effect of the deviation from spherical symmetry is the appearance of a non-trivial U(1) field y which can be evaluated perturbatively [33].

Since the current in the right hand side of the U(1) equation in (2.8) is proportional to g'^2, the U(1) amplitude y is also proportional to g'^2 in the lowest order, hence one can set

$$y(r,\vartheta) = \frac{g'^2\, r^2}{2g^2}\, p(r)\sin\vartheta \qquad \text{where} \qquad \left(r^4 p'\right)' = r^2(1-f)\phi^2. \tag{6.4}$$

Here the differential equation for $p(r)$ is obtained by injecting $y(r,\vartheta)$ to the field equations and keeping only the terms of order g'^2, whereas the f, ϕ amplitudes in this perturbative order are still described by Eqs.(4.21). The solution is such that for $0 \leftarrow r \to \infty$ one has

$$const. \leftarrow p(r) \to \frac{C}{r^3} \qquad \text{with} \qquad C = \frac{1}{3}\int_0^\infty r^2(f-1)\phi^2\, dr\,, \tag{6.5}$$

where the equation in (6.4) was used to evaluate C. The electromagnetic field (2.13) has the following non-zero components in the lowest in g' order,

$$F_{r\varphi} = \frac{g'}{2g}\left(2f' + (r^2 p)'\right)\sin^2\vartheta\,, \qquad F_{\vartheta\varphi} = \frac{g'}{g}(f^2 - 1 + r^2 p)\sin\vartheta\cos\vartheta\,. \tag{6.6}$$

Injecting this to (2.15) determines the magnetic charge and electric current densities,

$$\rho_{\rm SU(2)} = \frac{1}{4\pi}\frac{2g'}{gr^2}(f-1)f'\cos\vartheta, \qquad J_\varphi = -\frac{1}{4\pi}\frac{g'}{gr^2}(f^2-1)(f-1)\sin^2\vartheta\,. \tag{6.7}$$

Notice that $p(r)$ drops out from these expressions. Since $f = 1 + \mathcal{O}\left(e^{-m_{\rm W} r}\right)$ as $r \to \infty$, it follows that at large r one has

$$F = d\mathcal{A} \qquad \text{with} \qquad \mathcal{A} = \frac{g'C}{2rg}\sin^2\vartheta\, d\varphi = \frac{\vec{\mu}\wedge\vec{r}}{r^3}\,, \tag{6.8}$$

where the sphaleron magnetic moment is

$$\vec{\mu} = \vec{n}_z\,\frac{g'C}{2g} = \vec{n}_z\,\frac{g'}{6g}\int_0^\infty r^2(f-1)\phi^2 dr = \int\left(\rho_{\rm SU(2)}\,\vec{r} + \frac{1}{2}\,\vec{r}\wedge\vec{J}\right)d^3x\,, \tag{6.9}$$

with $\vec{n}_z$ being the unit vector along the z-axis. Here the first integral comes from (6.5), the second integral is the standard expression for the magnetic moment, and their equality can be checked by using (6.7) and the background equations (4.21) [33].

Therefore, the sphaleron magnetic moment receives a contribution from the azimuthal electric current and also from the magnetic charge distribution. The current attains its maximal value in the equatorial plane whereas the magnetic charge density changes sign through the plane. The total magnetic charge in the $z > 0$ region is

$$P = 2\pi \int_0^{\pi/2} \sin\vartheta \, d\vartheta \int_0^{\infty} \rho_{\mathrm{SU}(2)} \, r^2 \, dr = -\frac{g'}{g} \, , \tag{6.10}$$

and that in the $z < 0$ region is $+g'/g$. As a result, the perturbative analysis indicates that the sphaleron contains a pair of oppositely charged magnetic monopoles with charges $\pm g'/g$, encircled by an electric current [33].

We were able to confirm the above considerations at the non-perturbative level by drawing level surfaces for the magnetic charge density and for the electric current obtained from (2.15). The left part of Fig.12 presents the result for the fundamental $\nu = 1$ sphaleron (for $g'^2 = 0.23$), where one can clearly see the thick belt representing the equatorial azimuthal current (red online) surrounding two oppositely charged and separated in space monopoles (green and blue online). The mutual attraction of the monopoles is compensated by the magnetic field created by the current, while the current itself exists because the magnetic field created by the monopoles forces the electric charges to Larmore orbit along the azimuthal direction.

It is interesting that interchanging in this picture "magnetic charges $\leftrightarrow$ electric currents" yields the description of monopoles, because they contain inside oppositely directed currents and a magnetically charged ring, instead of opposite magnetic charges and a current. In this sense monopoles and sphalerons are mutually "dual". In both cases the Higgs field shows only one zero – at the origin.

What are the monopoles inside the sphaleron ? Their charges $\pm g'/g$ may correspond either to the monopole and antimonopole of Nambu, or to the SU(2) part of the charge of monopole and antimonopole of Cho-Maison. However, the total energy is finite, and in addition the distribution of the Z-field defined by (2.13) shows a Z-flux tube between the monopoles, hence they are connected through a vortex. Therefore, these must be the Nambu monopole and antimonopole [33]. Still, the relation to the Cho-Maison monopoles is stunning, since comparing the regularized energy of the $\nu = 2$ monopole solution with the energy of the $\nu = 1$ sphaleron yields almost the same values:

$$\nu = 1 \;\; \text{sphaleron} : \quad E = 38.473; \qquad \nu = 2 \;\; \text{monopole} : \quad E_{\mathrm{reg}} = 38.119. \tag{6.11}$$

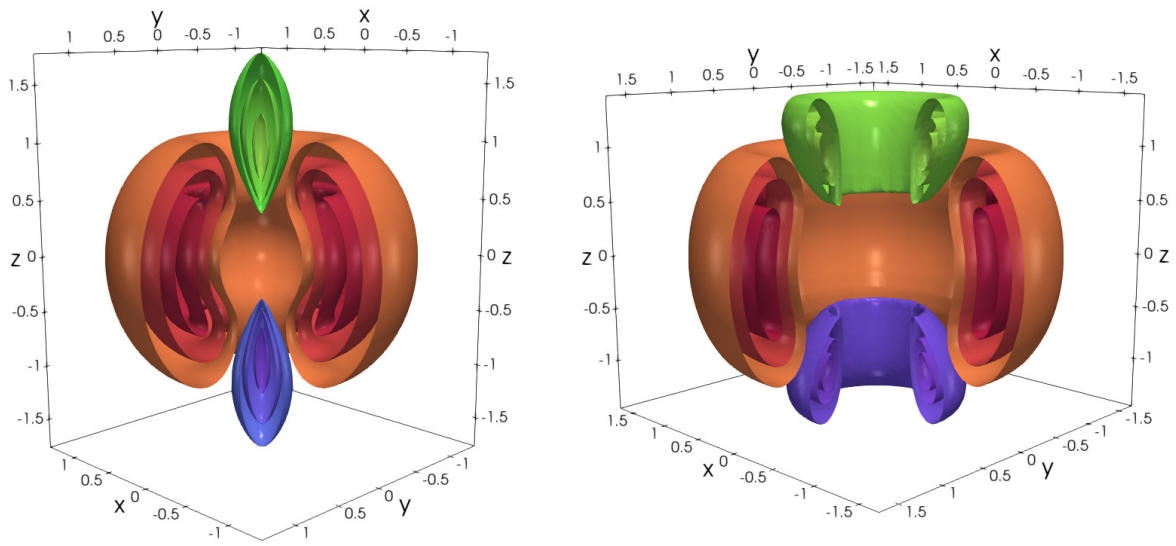


FIG. 12. Surfaces of constant magnetic charge and electric current densities for the $\nu = 1$ sphaleron (left) and for the $\nu = 2$ sphaleron (right).

Therefore, the regular part of the Cho-Maison monopole is similar to the Nambu monopole because they both have the same value of the magnetic charge and almost the same energy. Moreover, as seen in Fig.12, for $\nu = 2$ the sphaleron shows inside two magnetically charged rings. These must be the Nambu monopole and antimonopole with charges $\pm 2g'/g$. Therefore, for higher values of the charge the Nambu monopole contains inside a magnetic ring. At the same time, we know that the $\nu = \mp 2$ generalizations of the Cho-Maison monopole also contains inside a magnetic ring of charge $\pm 2g'/g$, respectively, which are the same values as for the Nambu monopole and antimonopole.

Summarizing, it seems that there exists a relation between monopoles of Nambu and monopoles of Cho-Maison. In some sense, the Nambu monopoles can be viewed as Cho-Maison monopoles with the divergent U(1) part removed. At the same time, the Nambu monopole is not an equilibrium configuration of the theory because it is attached to a semi-infinite vortex pulling it. The Nambu monopole-antimonopole pair inside the sphaleron is static but its total magnetic charge is zero. The only equilibrium non-Abelian configurations with a non-zero magnetic charge are the Cho-Maison monopole and its multi-charge generalizations.

VII. SUMMARY AND CONCLUDING REMARKS

To recapitulate, we have constructed the multi-charge generalizations for the non-Abelian electroweak monopole of Cho and Maison. The Cho-Maison monopole is spherically symmetric and has the magnetic charge $P = 1/e$ or $P = -1/e$ (for the monopole and antimonopole).

The new solutions are axially symmetric and exist for any value of P, but they are free of line singularities of the Dirac string type if only their magnetic charge is an integer multiple of $1/e$, hence $P = -\nu/e = -\nu\,(g/g' + g'/g) \equiv P_{\rm U(1)} + P_{\rm SU(2)}$ with $\nu \in \mathbb{Z}$. Far away from the center, the solutions become purely electromagnetic and approach fields of the Dirac magnetic monopole of charge P, while closer to the center they contain non-linear fields and a U(1) hypercharge field of Coulombian type. The latter makes an infinite contribution to the energy, but subtracting the Coulombian part renders the energy finite, and the remaining part of the system is completely regular. The U(1) contribution to the magnetic charge, $P_{\rm U(1)}$, is concentrated in the monopole center, while the SU(2) part of the charge, $P_{\rm SU(2)}$, is smoothly distributed over the volume of a ring of a finite thickness. The quantization of values of $P_{\rm SU(2)}$ is the same as for the Nambu monopole.

The multi-monopoles are characterized by a magnetic quadrupole moment that rapidly increases with growing magnetic charge. For large values of the charge, the monopoles are strongly squashed and their U(1) field becomes strong enough to suppress all other fields and restore the full gauge symmetry within a spheroidal central region – a bubble of symmetric phase of size $R \propto \sqrt{|P|}$. The bubble is encircled by a belt of broken phase containing the W-condensate in the form of a magnetically charged ring sandwiched between two superconducting rings of oppositely directed electric currents. This can be interpreted by saying that the magnetic ring creates the circular electric currents, while the latter produce a magnetic field that squeezes the individual CM monopoles into the magnetic ring. The magnetic ring gives the leading contribution to the quadrupole moment $q \approx |P_{\rm SU(2)}|R^2$.

It is interesting that exchanging "magnetic charges $\leftrightarrow$ electric currents" yields a qualitative description of the interior of sphalerons, so that monopoles and sphalerons are mutually "dual". It is also interesting that the structure of the regular part of the Cho-Maison monopole configuration is very similar to the Nambu monopoles inside the sphalerons.

The Cho-Maison maison is stable with respect to any (small) perturbations, hence it may be viewed as a remnant of decay of the Dirac monopole of the same charge [26]. The latter is unstable, but only with respect to spherically symmetric perturbations, hence it is conceivable that it radiates away a part of the energy, while the rest condenses to the spherically symmetric CM monopole. The Dirac monopole with ν units of the CM magnetic charge is also unstable, but only with respect to perturbations with angular momentum $j = |\nu| - 1$. One may therefore conjecture that its instability leads to a formation of a stable non-Abelian configuration which may have no symmetry at all or perhaps shows only discrete symmetries as for the spherical harmonics [26].

Our results provide a partial confirmation of the conjecture since the spherical harmonics $Y_{jm}(\vartheta, \varphi)$ become axially symmetric for $m = 0$. And indeed, we find axially symmetric non-Abelian solutions for higher values of the magnetic charge, although we could not yet prove that they are stable. However, they are presumably only a special case of more general, non-axially symmetric non-Abelian monopoles. In other words, the electroweak theory may admit many other not yet known non-Abelian monopole solutions.

It is likely that our solutions can be generalized to describe monopole-antimonopole pairs and monopole chains, as was the case for the t'Hooft-Polyakov monopoles [50, 51].

The total energy of all electroweak monopoles is always infinite due to the U(1) hypercharge field $B = \nu\,(\cos\vartheta \pm 1)d\varphi$ generated by the pointlike magnetic charge at the center, whose energy density $\nu^2/(2g'^2r^4)$ diverges at the origin. However, the divergence will be regularized when gravity is taken into account, which this should impose a cutoff via producing an event horizon to shield the singularity at $r = 0$ and render the energy finite. In fact, the gravitating generalization for the spherically symmetric Cho-Maison monopole is already known and is indeed described by a black hole geometry with a finite mass [25]. Similar black hole generalizations should exist also for axially symmetric monopoles. This is almost obvious for large charges when the monopoles show inside the bubble of symmetric phase containing only the spherically symmetric hypercharge field B. One can expect that switching the gravity on will replace the underlying Minkowski geometry in the bubble by the geometry of a static and spherically symmetric charged black hole, without affecting the B field. The minimal event horizon size will be of the order of $|\nu|/g'$ multiplied by the Planck length, which is many orders of magnitude less than the size of the bubble. Therefore, the presence of a small black hole in the center should not change anything in the bubble, nor should it affect the non-Abelian fields outside the bubble. In other words, the inner monopole structure with the bubble and rings shown in Fig.10 is expected to remain almost intact if the central pointlike charge is replaced by a small black hole of the same charge. Similar behaviour is known for the t'Hooft-Polyakov monopole and other solitons which can incorporate a small black hole in the center without essentially changing their form [52].

Summarizing, we expect that when coupled to gravity, the electroweak theory should admit magnetically charged "hairy" black holes which are either axially symmetric or have no continuous symmetries at all. The possible existence of such black holes was recently advocated by Maldacena [53], and before that, solutions of this type had been discussed at the perturbative level within a theory which is similar although not exactly identical to the electroweak theory [54–56]. However, such solutions have never been constructed explicitly. We therefore expect

that taking gravity into account should promote our multi-monopole solutions to static and axially symmetric hairy black holes with a finite mass.

Before finishing, one should say that non-Abelian monopoles in the electroweak theory were reported also in [57] (see also references therein) for the magnetic charge $P = 1/(2e)$, which is the least possible value in the Dirac picture. The same axially symmetric ansatz as in our case was used, assuming that at infinity the U(1) field is $B = (1/2) \times (\cos\vartheta \pm 1)d\varphi$, whose flux through the two-sphere is 2π. At the same time, it was assumed that B vanishes at the origin, and it was inferred from this that the energy is finite. However, the latter assumption is inconsistent with the former one since the flux of B is a topological invariant that does not depend on the size of the sphere, as seen in (3.16). Since its flux is conserved, B cannot vanish at the origin but should diverge there hence the energy should diverge as well. We therefore find unclear the status of the report.

ACKNOWLEDGEMENTS

The assistance of Julien Garaud in various issues concerning the FreeFem++ numerical solver was extremely helpful for us.

A. FAR FIELD ZONE

In this Appendix we analyze the asymptotic behaviour of solutions at spatial infinity, both for the monopoles and sphalerons. This shows in particular that the sphalerons have a magnetic dipole moment, whereas for the monopoles the asymptotic expansion starts from the quadrupole. This also shows that the gauge condition (3.20) used in our calculations gives rise to a spurious long-range mode of a pure gauge origin.

One has at large distances

$$F_1 = -\frac{1}{r}\,\delta H_1, \quad F_2 = \delta H_2, \quad F_3 = \Theta(\vartheta) + \delta H_3 \sin\vartheta, \quad F_4 = \delta H_4 \sin\vartheta,$$
$$Y = \Theta(\vartheta) + \delta y \, \sin\vartheta, \quad \phi_1 = \delta\phi_1, \quad \phi_2 = 1 + \delta\phi_2\,, \tag{A.1}$$

where the deviations $\delta H_1, \ldots, \delta\phi_2$ approach zero as $r \to \infty$ and where $\Theta(\vartheta) = \cos\vartheta$ in the monopole case while $\Theta(\vartheta) = 1$ in the sphaleron case. Since the deviations are small in the far field zone, the field equations can be linearized. It is convenient to use the original equations where the gauge is not fixed, then the linearized equations admit the gauge symmetry

$$\delta H_1 \to \delta H_1 - r\partial_r\chi, \quad \delta H_2 \to \delta H_2 + \partial_\vartheta\chi\,, \quad \delta H_4 \to \delta H_4 + \chi\,\frac{\Theta(\vartheta)}{\sin\vartheta}\,,$$
$$\delta\phi_1 \to \delta\phi_1 + \chi/2\,, \qquad \delta H_3 \to \delta H_3, \quad \delta y \to \delta y, \quad \delta\phi_2 \to \delta\phi_2\,, \tag{A.2}$$

which is obtained by assuming the gauge parameter χ in (3.3) to be small and linearizing.

1. Higgs sector

The linearized equation for $\delta\phi_2$ decouples from the others,

$$\left(\frac{\partial^2}{\partial r^2}+\frac{2}{r}\frac{\partial}{\partial r}+\frac{1}{r^2}\frac{\partial^2}{\partial\vartheta^2}+\frac{\cot\vartheta}{r^2}\frac{\partial}{\partial\vartheta}-\frac{\beta}{2}\right)\delta\phi_2=0, \tag{A.3}$$

which is solved by

$$\delta\phi_2=\frac{R_H(r)}{r}\,P_j(\cos\vartheta)\qquad\text{with}\qquad\left(\frac{d^2}{dr^2}-\frac{j(j+1)}{r^2}-\frac{\beta}{2}\right)R_H=0, \tag{A.4}$$

where $P_j(\cos\vartheta)$ are the Legendre polynomials. The orbital quantum number j can take any value $j=0,1,2,\ldots$, hence the general solution is a superposition of modes with different j, but the $j=0$ mode decays slower than other modes hence it is dominant at large r. Therefore, the leading contribution is described by the Yukawa potential,

$$\delta\phi_2=\frac{C_H}{r}\,e^{-m_{\rm H}\,r}\,, \tag{A.5}$$

where C_H is an integration constant and $m_{\rm H}$ is the Higgs boson mass defined in (2.11). This solution applies both for monopoles and sphalerons since in both cases one has $\partial_\vartheta\phi_2=0$ for $\vartheta=0$ and for $\vartheta=\pi/2$.

2. Electromagnetic and Z sectors

The equations for δH_3 and δy comprise a closed system, and setting $\delta y=y_\gamma+g'^2\,y_Z$ and $\delta H_3=y_\gamma-g^2y_Z$, the system splits into two independent equations,

$$\hat{\mathcal{D}}_1\,y_\gamma=0,\qquad\left(\hat{\mathcal{D}}_1\,-\frac{1}{2}\right)y_Z=0, \tag{A.6}$$

where the differential operator is defined by

$$\hat{\mathcal{D}}_m=\frac{\partial^2}{\partial r^2}+\frac{1}{r^2}\left(\frac{\partial^2}{\partial\vartheta^2}+\cot\vartheta\,\frac{\partial}{\partial\vartheta}-\frac{m^2}{\sin^2\vartheta}\right). \tag{A.7}$$

The eigenfunctions of the angular part of this operator are the associated Legendre polynomials $P_j^m(\cos\vartheta)$, the corresponding eigenvalue being $-j(j+1)$ with $j=|m|,|m|+1,\ldots$, hence the solution is

$$y_\gamma=R_\gamma(r)P_j^1(\cos\vartheta),\qquad y_Z=R_Z(r)P_j^1(\cos\vartheta). \tag{A.8}$$

Here $j=1,2,\ldots$ and

$$\left(\frac{d^2}{dr^2}-\frac{j(j+1)}{r^2}\right)R_\gamma=0,\qquad\left(\frac{d^2}{dr^2}-\frac{j(j+1)}{r^2}-\frac{1}{2}\right)R_Z=0. \tag{A.9}$$

This describes the massless electromagnetic and massive Z modes, and this solution applies both to monopoles and sphalerons. However, the allowed values of j are not the same in both cases since the boundary conditions are different.

For the sphalerons one should have $y = H_3 = 0$ at $\vartheta = 0$ and $\partial_\vartheta y = \partial_\vartheta H_3 = 0$ at $\vartheta = \pi/2$, hence one can choose the minimal value of the angular momentum, $j = 1$, which gives the dominant at infinity solution

$$\underline{\text{sphalerons}}: \qquad y_\gamma = \frac{C_\gamma}{r}\,\sin\vartheta\,, \qquad y_Z = C_Z\, e^{-m_Z r}\,\sin\vartheta\, + \ldots\,, \tag{A.10}$$

with the dots denoting subleading terms. The electromagnetic mode y_γ describes the magnetic dipole moment.

For the monopoles one should have $y = H_3 = 0$ both for $\vartheta = 0$ and $\vartheta = \pi/2$, hence one cannot have $j = 1$ so that the dipole moment is zero. The minimal possible value is $j = 2$, which defines the leading behaviour

$$\underline{\text{monopoles}}: \qquad y_\gamma = \frac{C_\gamma}{r^2}\,\sin\vartheta\cos\vartheta\,, \qquad y_Z = C_Z\, e^{-m_Z r}\,\sin\vartheta\cos\vartheta\, + \ldots\,, \tag{A.11}$$

and this corresponds to the magnetic quadrupole moment.

3. W sector

The four amplitudes $\delta H_1, \delta H_2, \delta H_4, \delta\phi_1$ fulfill a system of four equations admitting the gauge symmetry (A.2). This symmetry can be used to impose the condition $\delta\phi_1 = 0$, which corresponds to the unitary gauge. The subsequent steps are slightly different for monopoles and for sphalerons.

a. Monopoles

The four equations for $\delta H_1, \delta H_2, \delta H_4, \delta\phi_1$ with $\delta\phi_1 = 0$ are solved by setting

$$\begin{aligned}
\delta H_1 &= \nu\,\frac{f_1(r)}{r}\,P_j^\nu(\cos\vartheta)\,,\\
\delta H_2 &= \nu f_3(r) P_j^{\nu-1}(\cos\vartheta) + \nu f_2(r) P_j^{\nu+1}(\cos\vartheta)\,,\\
\delta H_4 &= f_3(r) P_j^{\nu-1}(\cos\vartheta) - f_2(r) P_j^{\nu+1}(\cos\vartheta)\,.
\end{aligned} \tag{A.12}$$

Using the recurrence relations

$$(\partial_\vartheta \mp m\cot\vartheta) P_j^m(\cos\vartheta) = \lambda_\pm P_j^{m\pm1}(\cos\vartheta)\,, \tag{A.13}$$

with $\lambda_+ = 1$ and $\lambda_- = m(m-1) - j(j+1)$, the angular dependence separates. The equations for $f_1(r)$ and $f_2(r)$ become

$$\left(\frac{d^2}{dr^2} + \frac{\nu^2 - j(j+1)}{r^2} - \frac{g^2}{2}\right) f_1 = 0\,,$$
$$\left(\frac{d^2}{dr^2} + \frac{\nu^2 - j(j+1)}{r^2} - \frac{g^2}{2}\right) f_2 = \frac{f_1}{r^3}\,, \tag{A.14}$$

and the remaining equations reduce to the constraint

$$f_3 = f_1' + (j-\nu)(j+1+\nu) f_2\,. \tag{A.15}$$

Denoting $C_W^{(1)}$ and $C_W^{(2)}$ two integration constants, one obtains from (A.14)

$$f_1 = C_W^{(1)}\, e^{-m_{\rm W}\, r} + \dots\,, \qquad f_2 = C_W^{(2)}\, e^{-m_{\rm W}\, r} + \dots\,. \tag{A.16}$$

This solution describes massive W boson modes.

Summarizing, all field amplitudes approach their asymptotic values exponentially fast, apart from δH_3 and δy which decay as $1/r^2$. This agrees with properties of the perturbative states in the theory. However, this behaviour is manifest only in the unitary gauge, while the gauge (3.20) used for the numerical integration is not unitary. Solving the linearized equations in this gauge as was done above yields the same solutions for $\delta\phi_2$, δH_3, δy since these amplitudes are gauge invariant, but the gauge-dependent amplitudes $\delta H_1, \delta H_2, \delta H_4, \delta\phi_1$ then look completely different,

$$\delta H_1 = \frac{A}{r^2}\sin(2\vartheta) + \dots\,, \quad \delta H_2 = \frac{A}{r^2}\cos(2\vartheta) + \dots\,,$$
$$\delta H_4 = \frac{A}{r^2}\cos^2\vartheta + \dots\,, \quad \delta\phi_1 = \frac{A}{4r^2}\sin(2\vartheta) + \dots\,. \tag{A.17}$$

Here A is an integration constant and the dots denote subleading terms containing the exponentially small massive modes described by (A.11), (A.16). As a result, the solution shows a second long-range tail in addition to the electromagnetic one. Of course, this additional mode is pure gauge and can be removed by the gauge transformation (A.2) with the gauge parameter

$$\chi = -2\delta\phi_1 = -\frac{A}{2r^2}\sin(2\vartheta) + \dots\,, \tag{A.18}$$

which is equivalent to setting $A = 0$ in (A.17). However, this mode appears in the numerical integration procedure as a result of the gauge condition (3.20). One might try to exclude this spurious mode by choosing some other gauge, as for example the unitary gauge. However, as shown below in Appendix B, the unitary gauge is singular at the origin, whereas the gauge (3.20) is globally regular, which is why it is preferable, even though it produces the spurious mode at infinity.

b. Sphalerons

Curiously, the linearized equations do not admit a complete separation of variables in this case. Passing to the unitary gauge $\delta\phi_1 = 0$, the four equations for $\delta H_1, \delta H_2, \delta H_4, \delta\phi_1$ reduce to three independent ones, of which one decouples and is solved by

$$\delta H_1 = \frac{f_1(r)}{r} P_j^\nu(\cos\vartheta)\,, \qquad \left(\frac{d^2}{dr^2} - \frac{j(j+1)}{r^2} - \frac{g^2}{2}\right) f_1 = 0\,. \tag{A.19}$$

The solution enters the equation for δH_2 as a source term,

$$\left(\hat{\mathcal{D}}_\nu - \frac{g^2}{2}\right)(\sin\vartheta\,\delta H_2) = \frac{2}{r^2}\left(\cot\vartheta\; r\,\frac{\partial}{\partial r} + \frac{\partial}{\partial\vartheta}\right)\sin\vartheta\,\delta H_1\,, \tag{A.20}$$

while δH_4 is determined algebraically,

$$\nu^2\delta H_4 = \partial_\vartheta(\sin\vartheta\,\delta H_2) - \sin\vartheta\,\partial_r(r\delta H_1). \tag{A.21}$$

These equations admit two independent solutions decaying as $e^{-m_{\rm W} r}$ at large r. Therefore, the far field solution is a superposition of short-range massive modes and a long-range electromagnetic mode. This behaviour is manifest in the unitary gauge, while in the gauge (3.20) used for numerical integration the gauge-dependent amplitudes $\delta H_1, \delta H_2, \delta H_4, \delta\phi_1$ show a long-range spurious mode similar to (A.17) for the monopoles.

B. SOLUTION AT THE ORIGIN

In this Appendix we analyze the behaviour of the solutions for small r, close to the origin $r = 0$. The complete analysis turns out to be rather involved, and we shall consider only the behaviour of the Higgs field in the monopole case, which will lead to important conclusions.

Close to the origin the monopole fields approach

$$H_1 = H_3 = y = \phi_1 = \phi_2 = 0, \qquad H_2 = H_4 = 1, \tag{B.1}$$

which can be called "false vacuum". This is an exact solution of the equations for any r, ϑ, but the monopole fields approach it only for $r \to 0$. Therefore, for small r one has

$$\begin{aligned} &H_1 = \delta H_1, \quad H_2 = 1 + \delta H_2, \quad H_3 = \delta H_3, \quad H_4 = 1 + \delta H_4, \\ &y = \delta y, \qquad \phi_1 = \delta\phi_1, \qquad \phi_2 = \delta\phi_2\,, \end{aligned} \tag{B.2}$$

where the deviations $\delta H_1, \ldots, \delta\phi_2$ vanish in the $r \to 0$ limit. Injecting this to the field equations and linearizing with respect to the deviations, it turns out that the equations for $\delta\phi_1$ and $\delta\phi_2$ decouple from the rest. One can neglect in these two equations terms proportional

to the Higgs coupling β since they are small as compared to the other terms if r is small. After this, the equations become homogeneous in r and setting

$$\delta\phi_1 = r^\lambda\, S_1(\vartheta), \qquad \delta\phi_2 = r^\lambda\, S_2(\vartheta), \tag{B.3}$$

the variables separate and the equations reduce to

$$\left(\lambda(\lambda+1) + \frac{d^2}{d\vartheta^2} + \cot\vartheta\,\frac{d}{d\vartheta} - \frac{\nu^2}{\sin^2\vartheta} + \frac{3\nu^2-1}{4}\right) S_1 - \left(\frac{d}{d\vartheta} + \frac{1-\nu^2}{2}\,\cot\vartheta\right) S_2 = 0,$$
$$\left(\lambda(\lambda+1) + \frac{d^2}{d\vartheta^2} + \cot\vartheta\,\frac{d}{d\vartheta} - \frac{\nu^2+1}{4}\right) S_2 + \left(\frac{d}{d\vartheta} + \frac{1+\nu^2}{2}\,\cot\vartheta\right) S_1 = 0. \tag{B.4}$$

This defines the eigenvalue problem to determine λ.

If $|\nu| = 1$ then setting $S_1 = 0$, $S_2 = const.$, the equations reduce to

$$\lambda(\lambda+1) - \frac{1}{2} = 0 \qquad \Rightarrow \qquad \lambda = \frac{\sqrt{3}-1}{2}\,, \tag{B.5}$$

which reproduces the small r behaviour of the CM monopole. If $|\nu| \neq 1$ then the solution is obtained by choosing (assuming that $\nu > 0$)

$$\lambda = \frac{\sqrt{1+2\nu}-1}{2}\,, \qquad S_1(\vartheta) = -\frac{2}{\nu+1}\,\frac{d}{d\vartheta}\,S_2(\vartheta)\,. \tag{B.6}$$

This formula determines the rate with which the Higgs field approaches zero at the origin. Using this, Eqs.(B.4) reduce to

$$\left(\frac{d^2}{d\vartheta^2} - \nu\cot\vartheta\,\frac{d}{d\vartheta} + \frac{1-\nu^2}{4}\right) S_2 = 0, \tag{B.7}$$

whose solution is

$$S_2(\vartheta) = \left(\sin\frac{\vartheta}{2}\right)^{\nu+1} + \left(\cos\frac{\vartheta}{2}\right)^{\nu+1}. \tag{B.8}$$

Since the derivative $dS_2(\vartheta)/d\vartheta$ vanishes for $\vartheta = 0$ and for $\vartheta = \pi/2$, the deviations $\delta\phi_1$ and $\delta\phi_2$ satisfy the correct boundary conditions at the symmetry axis and in the equatorial plane.

This result has an interesting consequence. The gauge transformation (3.3) changes the Higgs amplitudes as

$$\delta\phi_1 \to \delta\tilde\phi_1 = \delta\phi_1\,\cos\frac{\chi}{2} + \delta\phi_2\,\sin\frac{\chi}{2},$$
$$\delta\phi_2 \to \delta\tilde\phi_2 = \delta\phi_2\,\cos\frac{\chi}{2} - \delta\phi_1\,\sin\frac{\chi}{2}, \tag{B.9}$$

and if we require the new gauge to be unitary, $\delta\tilde\phi_1 = 0$, this implies that

$$\tan\frac{\chi}{2} = -\frac{\delta\phi_1}{\delta\phi_2} = -\frac{S_1(\vartheta)}{S_2(\vartheta)}. \tag{B.10}$$

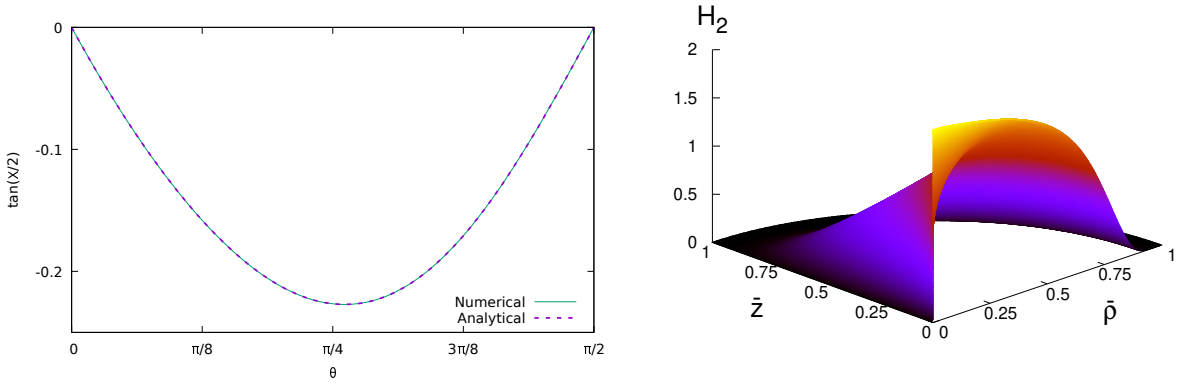


FIG. 13. Left: plots of $\tan(\chi/2)$ analytically obtained from (B.10) and also numerically from (B.11) for $r \to 0$. The two plots exactly coincide to each other and determine the $r \to 0$ limit of the gauge transformation toward the unitary gauge. Right: the H_2 amplitude of the $\nu = 2$ solution transformed to the unitary gauge.

This determines the $r \to 0$ limit of the parameter χ of the gauge transformation putting the solution to the unitary gauge. Notice that although $\delta\phi_1$ and $\delta\phi_2$ are small near the origin, their ratio and hence the gauge parameter χ are not small.

This fact can be used to check the quality of our numerical solutions obtained in the gauge (3.20). In order to transform a given solution to the unitary gauge, one should perform the gauge transformation (3.3) with the parameter

$$\tan\frac{\chi}{2} = -\frac{\phi_1}{\phi_2}\,, \tag{B.11}$$

where ϕ_1 and ϕ_2 are numerically obtained functions of r, ϑ. This gauge parameter should agree for small r with the one in (B.10) for the procedure to be consistent, and this is indeed the case. In Fig.13 we plot $\tan(\chi/2)$ given by the analytical formula (B.10) and also $\tan(\chi/2)$ numerically obtained from (B.11) in the $r \to 0$ limit, and the two plots exactly coincide to each other so that only one curve can be seen in Fig.13. Therefore, our procedure is consistent.

The same gauge transformation changes the false vacuum configuration (B.1) to

$$\begin{aligned} &H_1 = 0, \qquad H_2 = 1 + \frac{d\chi}{d\vartheta}\,, \qquad y = \phi_1 = \phi_2 = 0, \\ &H_3 = (\cos\chi - 1)\cot\vartheta - \sin\chi\,, \qquad H_4 = \cos\chi + \sin\chi\cot\vartheta\,, \end{aligned} \tag{B.12}$$

which is the $r \to 0$ limit of the solution expressed in the unitary gauge. Notice however that this limit is ϑ-dependent since χ in (B.10) depends on ϑ. On the other hand, nothing should depend on ϑ there because $r = 0$ is a single point in space. To illustrate this, Fig.13 shows H_2 for the $\nu = 2$ solution, the same as in Fig.3, but transformed to the unitary gauge. As seen,

H_2 does not have a definite limit at the origin $\bar{\rho} = \bar{z} = 0$ but assumes there all values from the interval $[0 : 2]$, depending on the direction the origin is approached. This agrees with (B.12) since one has at the origin $H_2 = 1 + d\chi/d\vartheta$ where the derivative of $\chi(\vartheta)$ defined in (B.10) varies in the interval $[-1 : 1]$.

Therefore, the unitary gauge is singular at small r, although it is well adapted to describe the large r region. On the other hand, the gauge (3.20) is regular everywhere but exhibits the spurious long-range mode (A.17) at large r.

---

[1] P. A. M. Dirac, *Quantised singularities in the electromagnetic field,*, *Proc. Roy. Soc. Lond. A* **133** (1931), no. 821 60–72, [doi:10.1098/rspa.1931.0130].

[2] T. T. Wu and C. N. Yang, *Dirac monopole without strings: monopole harmonics*, *Nucl. Phys. B* **107** (1976) 365, [doi:10.1016/0550-3213(76)90143-7].

[3] G. 't Hooft, *Magnetic monopoles in unified gauge theories*, *Nucl. Phys. B* **79** (1974) 276–284, [doi:10.1016/0550-3213(74)90486-6].

[4] A. M. Polyakov, *Particle spectrum in quantum field theory*, *JETP Lett.* **20** (1974) 194–195.

[5] P. Goddard and D. I. Olive, *New developments in the theory of magnetic monopoles*, *Rept. Prog. Phys.* **41** (1978) 1357, [doi:10.1088/0034-4885/41/9/001].

[6] S. R. Coleman, *The magnetic monopole fifty years later*, in *Les Houches Summer School of Theoretical Physics: Laser-Plasma Interactions*, pp. 461–552, 6, 1982.

[7] K. Konishi, *The magnetic monopoles seventy-five years later*, *Lect. Notes Phys.* **737** (2008) 471–521, [arXiv:hep-th/0702102].

[8] N. S. Manton and P. Sutcliffe, *Topological solitons*. Cambridge Monographs on Mathematical Physics. Cambridge University Press, 2004.

[9] Y. M. Shnir, *Magnetic Monopoles*. Text and Monographs in Physics. Springer, Berlin/Heidelberg, 2005.

[10] A. H. Chamseddine and M. S. Volkov, *NonAbelian BPS monopoles in N=4 gauged supergravity*, *Phys. Rev. Lett.* **79** (1997) 3343–3346, [arXiv:hep-th/9707176], [doi:10.1103/PhysRevLett.79.3343].

[11] P. Forgacs and M. S. Volkov, *Resonant excitations of the 't Hooft-Polyakov monopole*, *Phys. Rev. Lett.* **92** (2004) 151802, [arXiv:hep-th/0311062], [doi:10.1103/PhysRevLett.92.151802].

[12] A. Rajantie, *The search for magnetic monopoles*, *Phys. Today* **69** (2016), no. 10 40–46, [doi:10.1063/PT.3.3328].

[13] V. A. Mitsou, *Searches for magnetic monopoles: a review*, *MDPI Proc.* **13** (2019), no. 1 10, [doi:10.3390/proceedings2019013010].

[14] N. E. Mavromatos and V. A. Mitsou, *Magnetic monopoles revisited: Models and searches at colliders and in the Cosmos*, *Int. J. Mod. Phys. A* **35** (2020), no. 23 2030012, [arXiv:2005.05100], [doi:10.1142/S0217751X20300124].

[15] Y. Nambu, *String-like configurations in the Weinberg-Salam theory*, *Nucl. Phys. B* **130** (1977) 505, [doi:10.1016/0550-3213(77)90252-8].

[16] A. A. Abrikosov, *On the Magnetic properties of superconductors of the second group*, *Sov. Phys. JETP* **5** (1957) 1174–1182.

[17] H. B. Nielsen and P. Olesen, *Vortex Line Models for Dual Strings*, *Nucl. Phys. B* **61** (1973) 45–61, [doi:10.1016/0550-3213(73)90350-7].

[18] J. Urrestilla, A. Achucarro, J. Borrill, and A. R. Liddle, *The evolution and persistence of dumbbells in electroweak theory*, *JHEP* **08** (2002) 033, [arXiv:hep-ph/0106282], [doi:10.1088/1126-6708/2002/08/033].

[19] Y. M. Cho and D. Maison, *Monopoles in Weinberg-Salam model*, *Phys. Lett. B* **391** (1997) 360–365, [arXiv:hep-th/9601028], [doi:10.1016/S0370-2693(96)01492-X].

[20] Y. M. Cho, K. Kim, and J. H. Yoon, *Finite energy electroweak dyon*, *Eur. Phys. J. C* **75** (2015), no. 2 67, [arXiv:1305.1699], [doi:10.1140/epjc/s10052-015-3290-3].

[21] D. G. Pak, P. M. Zhang, and L. P. Zou, *On finite energy monopole solutions in Weinberg–Salam model*, *Int. J. Mod. Phys. A* **30** (2015), no. 27 1550164, [arXiv:1311.7567], [doi:10.1142/S0217751X1550164X].

[22] F. Blaschke and P. Beneš, *BPS Cho–Maison monopole*, *PTEP* **2018** (2018), no. 7 073B03, [arXiv:1711.04842], [doi:10.1093/ptep/pty071].

[23] J. Ellis, P. Q. Hung, and N. E. Mavromatos, *An electroweak monopole, Dirac quantization and the weak mixing angle*, *Nucl. Phys. B* **969** (2021) 115468, [arXiv:2008.00464], [doi:10.1016/j.nuclphysb.2021.115468].

[24] P. Q. Hung, *Topologically stable, finite-energy electroweak-scale monopoles*, *Nucl. Phys. B* **962** (2021) 115278, [arXiv:2003.02794], [doi:10.1016/j.nuclphysb.2020.115278].

[25] Y. Bai and M. Korwar, *Hairy magnetic and dyonic black holes in the Standard Model*, *JHEP* **04** (2021) 119, [arXiv:2012.15430], [doi:10.1007/JHEP04(2021)119].

[26] R. Gervalle and M. S. Volkov, *Electroweak monopoles and their stability*, *Nucl. Phys. B* **984** (2022) 115937, [arXiv:2203.16590], [doi:10.1016/j.nuclphysb.2022.115937].

[27] B. Kleihaus, J. Kunz, and Y. Brihaye, *The electroweak sphaleron at physical mixing angle*,

Phys. Lett. B **273** (1991) 100–104, [doi:10.1016/0370-2693(91)90560-D].

[28] J. Kunz, B. Kleihaus, and Y. Brihaye, *Sphalerons at finite mixing angle*, *Phys. Rev. D* **46** (1992) 3587–3600, [doi:10.1103/PhysRevD.46.3587].

[29] R. F. Dashen, B. Hasslacher, and A. Neveu, *Nonperturbative methods and extended hadron models in field theory. 3. Four-dimensional nonabelian models*, *Phys. Rev. D* **10** (1974) 4138, [doi:10.1103/PhysRevD.10.4138].

[30] L. G. Yaffe, *Static solutions of SU(2) Higgs theory*, *Phys. Rev. D* **40** (1989) 3463, [doi:10.1103/PhysRevD.40.3463].

[31] M. E. R. James, *The Sphaleron at nonzero Weinberg angle*, *Z. Phys. C* **55** (1992) 515–524, [doi:10.1007/BF01565115].

[32] F. R. Klinkhamer and N. S. Manton, *A saddle point solution in the Weinberg-Salam theory*, *Phys. Rev. D* **30** (1984) 2212, [doi:10.1103/PhysRevD.30.2212].

[33] M. Hindmarsh and M. James, *The origin of the sphaleron dipole moment*, *Phys. Rev. D* **49** (1994) 6109–6114, [arXiv:hep-ph/9307205], [doi:10.1103/PhysRevD.49.6109].

[34] F. Hecht, *New development in freefem++*, *J. Numer. Math.* **20** (2012), no. 3-4 251–265.

[35] C. Rebbi and P. Rossi, *Multi - Monopole Solutions in the Prasad-sommerfield Limit*, *Phys. Rev. D* **22** (1980) 2010, [doi:10.1103/PhysRevD.22.2010].

[36] B. Kleihaus and J. Kunz, *Static axially symmetric Einstein Yang-Mills dilaton solutions: 1. Regular solutions*, *Phys. Rev. D* **57** (1998) 834–856, [arXiv:gr-qc/9707045], [doi:10.1103/PhysRevD.57.834].

[37] B. Kleihaus, J. Kunz, and M. Leissner, *Sphalerons, Antisphalerons and Vortex Rings*, *Phys. Lett. B* **663** (2008) 438–444, [arXiv:0802.3275], [doi:10.1016/j.physletb.2008.04.027].

[38] B. Kleihaus, J. Kunz, and M. Leissner, *Electroweak Sphalerons with Spin and Charge*, *Phys. Lett. B* **678** (2009) 313–316, [arXiv:0810.1142], [doi:10.1016/j.physletb.2009.06.045].

[39] R. Ibadov, B. Kleihaus, J. Kunz, and M. Leissner, *Rotating Electroweak Sphaleron-Antisphaleron Systems*, *Phys. Lett. B* **686** (2010) 298–306, [arXiv:1001.3027], [doi:10.1016/j.physletb.2010.02.058].

[40] Y. Yang, *Solitons in Field Theory and Nonlinear Analysis*. Springer, 2014.

[41] J. Ambjorn and P. Olesen, *A Condensate Solution of the Electroweak Theory Which Interpolates Between the Broken and the Symmetric Phase*, *Nucl. Phys. B* **330** (1990) 193–204, [doi:10.1016/0550-3213(90)90307-Y].

[42] J. Garaud and M. S. Volkov, *Superconducting non-Abelian vortices in Weinberg-Salam theory – electroweak thunderbolts*, *Nucl. Phys. B* **826** (2010) 174–216, [arXiv:0906.2996],

[doi:10.1016/j.nuclphysb.2009.10.003].

[43] R. Raab, O. De Lange, O. de Lange, and O. U. Press, *Multipole Theory in Electromagnetism: Classical, Quantum, and Symmetry Aspects, with Applications*. International Series of Monographs on Physics. OUP Oxford, 2005.

[44] J. Ambjorn and P. Olesen, *On electroweak magnetism*, *Nucl. Phys. B* **315** (1989) 606–614, [doi:10.1016/0550-3213(89)90004-7].

[45] J. Ambjorn and P. Olesen, *Electroweak Magnetism: Theory and Application*, *Int. J. Mod. Phys. A* **5** (1990) 4525–4558, [doi:10.1142/S0217751X90001914].

[46] B. Kleihaus and J. Kunz, *Multi - sphalerons in the weak interactions*, *Phys. Lett. B* **329** (1994) 61–67, [arXiv:hep-ph/9403289], [doi:10.1016/0370-2693(94)90517-7].

[47] B. Kleihaus and J. Kunz, *Multi - sphalerons in the Weinberg-Salam theory*, *Phys. Rev. D* **50** (1994) 5343–5351, [arXiv:hep-ph/9405387], [doi:10.1103/PhysRevD.50.5343].

[48] F. R. Klinkhamer, *Construction of a new electroweak sphaleron*, *Nucl. Phys. B* **410** (1993) 343–354, [arXiv:hep-ph/9306295], [doi:10.1016/0550-3213(93)90437-T].

[49] E. Radu and M. S. Volkov, *Spinning Electroweak Sphalerons*, *Phys. Rev. D* **79** (2009) 065021, [arXiv:0810.0908], [doi:10.1103/PhysRevD.79.065021].

[50] B. Kleihaus, J. Kunz, and Y. Shnir, *Monopoles, antimonopoles and vortex rings*, *Phys. Rev. D* **68** (2003) 101701, [arXiv:hep-th/0307215], [doi:10.1103/PhysRevD.68.101701].

[51] B. Kleihaus, J. Kunz, and Y. Shnir, *Monopole-antimonopole chains and vortex rings*, *Phys. Rev. D* **70** (2004) 065010, [arXiv:hep-th/0405169], [doi:10.1103/PhysRevD.70.065010].

[52] M. S. Volkov and D. V. Gal'tsov, *Gravitating nonAbelian solitons and black holes with Yang-Mills fields*, *Phys. Rept.* **319** (1999) 1–83, [arXiv:hep-th/9810070], [doi:10.1016/S0370-1573(99)00010-1].

[53] J. Maldacena, *Comments on magnetic black holes*, *JHEP* **04** (2021) 079, [arXiv:2004.06084], [doi:10.1007/JHEP04(2021)079].

[54] S. A. Ridgway and E. J. Weinberg, *Instabilities of magnetically charged black holes*, *Phys. Rev. D* **51** (1995) 638–646, [arXiv:hep-th/9409013], [doi:10.1103/PhysRevD.51.638].

[55] S. A. Ridgway and E. J. Weinberg, *Static black hole solutions without rotational symmetry*, *Phys. Rev. D* **52** (1995) 3440–3456, [arXiv:gr-qc/9503035], [doi:10.1103/PhysRevD.52.3440].

[56] S. A. Ridgway and E. J. Weinberg, *Are all static black hole solutions spherically symmetric?*, *Gen. Rel. Grav.* **27** (1995) 1017–1021, [arXiv:gr-qc/9504003], [doi:10.1007/BF02148644].

[57] R. Teh, B.-L. Ng, and K.-M. Wong, *Half-monopole in the Weinberg–Salam model*, *Annals Phys.* **354** (2015) 489–498, [arXiv:1406.0978], [doi:10.1016/j.aop.2015.01.018].